



**Escola de Camins**

Escola Tècnica Superior d'Enginyeria de Camins, Canals i Ports  
UPC BARCELONATECH

# TESI DE MÀSTER

**Màster**

**Enginyeria Civil**

**Títol**

**Nonlinear analysis of steel-concrete composite beams with full and partial shear connection**

**Autor**

**Cristian V. MICULAȘ**

**Tutor**

**prof. Enrique MIRAMBELL ARRIZABALAGA**

**Intensificació**

**Steel Structures**

**Data**

**July, 2015**



# Acknowledgment

First of all I would like to express my deepest gratitude to my supervisor, prof. Enrique Mirambell for his excellent guidance, caring, patience and for making me part of his excellent research team as well as for sharing his impressive knowledge, in the field of structural engineering, with me during my time at UPC.

Thanks also to prof. Cosmin G. Chiorean, under whose supervision I started my research at UTCN, for giving me the opportunity to develop this research and for his continuous support and interest throughout the project.

I would also like to express my sincere thanks to prof. Alex H. Barbat, for facilitating the collaboration between my supervisors.

Thanks also to Alexandru Chira and Ștefan M. Buru for guiding my research for the past several years and for helping me develop my background in the finite element method.

Further on, I would like to thank Itsaso Arrayago, Ovidiu Prodan and Tudor Milchiș for their friendship and advice.

Last but not least, I would like to express my deepest appreciation to my family and relatives for their support and understanding during this period of my life.



## ***Abstract english***

The present study proposes a numerical procedure for the analysis of steel and concrete composite beams with full and partial shear connection. The program accounts for nonlinear behavior of concrete slab, reinforcement, structural steel and shear connectors. The finite element models are adjusted, compared and validated with the corresponding experimental results and other numerical studies done by other researchers. The obtained results demonstrate that the numerical approach is a valid tool for extensive parametric studies on composite beams with full or partial shear connection. Finally, parametric analyses focusing on the influence of the slab concrete strength and width and the effects of fracture energy on the composite beam response are presented.

*Keywords:* steel-concrete composite structures, partial shear interaction, nonlinear analysis, finite element method, concrete slab composite effects.



## **Abstract *spanish***

El presente estudio propone un procedimiento numérico para el análisis de vigas mixtas hormigón-acero teniendo en cuenta el grado de conexión de la interficie frente a rasante longitudinal (conexión total vs. conexión parcial). El modelo numérico desarrollado considera el comportamiento no lineal de la losa de hormigón, de la armadura pasiva embebida en la losa de hormigón, del acero estructural y de los conectadores. Los modelos numéricos de elementos finitos desarrollados en este estudio se comparan y validan con resultados experimentales y con otros resultados analíticos y numéricos realizados por otros autores. Los resultados obtenidos demuestran que el modelo numérico empleado es una herramienta válida para la realización de amplios estudios paramétricos sobre el comportamiento estructural de vigas mixtas con conexión total y con conexión parcial. Por último, se presentan y analizan los resultados de diferentes estudios paramétricos llevados a cabo en el marco del presente trabajo para analizar la influencia de la resistencia del hormigón de la losa, de su ancho eficaz y de su energía de fractura en el comportamiento estructural de las vigas mixtas hormigón-acero.

*Palabras clave:* estructuras mixtas hormigón-acero, conexión parcial, análisis no lineal, método de los elementos finitos, influencia de la losa del hormigón.





# Contents

- Acknowledgement** **i**
- Abstract - english** **iii**
- Abstract - spanish** **v**
- List of Figures** **ix**
- List of Tables** **xi**
- 1 Introduction** **1**
  - 1.1 General aspects . . . . . 1
  - 1.2 Objectives . . . . . 2
  - 1.3 Structure and contents of the thesis . . . . . 3
- 2 State of the art review** **5**
  - 2.1 Introduction . . . . . 5
  - 2.2 Experimental results . . . . . 5
  - 2.3 Numerical results . . . . . 10
  - 2.4 Design prescriptions . . . . . 11
- 3 Finite element model** **17**
  - 3.1 Introduction . . . . . 17
  - 3.2 Geometry of the analyzed structures . . . . . 17
    - 3.2.1 General aspects . . . . . 17
    - 3.2.2 Element types and mesh construction . . . . . 18
  - 3.3 Material modeling . . . . . 20
    - 3.3.1 Concrete and reinforcing steel . . . . . 20
    - 3.3.2 Structural steel . . . . . 22
    - 3.3.3 Stud shear connectors . . . . . 24
  - 3.4 Non-linear analysis . . . . . 25
  - 3.5 Validation of the numerical model . . . . . 25
    - 3.5.1 Specimen E1, tested by Chapman *et al.* 1964 . . . . . 25
    - 3.5.2 Specimens SCB-1 and SCB-3, tested by Nie and Cai 2003 . . . . . 28
- 4 Parametric studies** **31**
  - 4.1 Attainment of full shear connection according to different design codes . . . . . 31
    - 4.1.1 Europe - EN 1994-1-1 2004 . . . . . 31
    - 4.1.2 Australia - AS-2327.1 2003 . . . . . 32
    - 4.1.3 United States of America - AISC-LRFD 1994 . . . . . 34
    - 4.1.4 Differences between the design codes . . . . . 35

## Contents

---

4.2	Influence of the slab concrete strength on the composite beam response . . . . .	36
4.3	Influence of the slab concrete width on the composite beam response . . . . .	37
4.4	Mesh-sensitivity analysis . . . . .	38
4.5	Fracture energy effects . . . . .	39
4.5.1	Computational effort . . . . .	43
<b>5</b>	<b>Conclusions and future lines of investigations</b>	<b>45</b>
5.1	Summary of the work . . . . .	45
5.2	Conclusions . . . . .	46
5.3	Future lines of investigation . . . . .	47
	<b>Bibliography</b>	<b>49</b>

# List of Figures

2.1	Test setup (Culver <i>et al.</i> 1961). . . . .	5
2.2	Test setup (Chapman <i>et al.</i> 1964). . . . .	7
2.3	Test setup (Loh <i>et al.</i> 2003a). . . . .	8
2.4	Web and flange buckling (Loh <i>et al.</i> 2003a). . . . .	9
2.5	Failure of stud connector (Loh <i>et al.</i> 2003a). . . . .	9
2.6	Concrete crushing and profiled steel sheeting buckling at mid-span (Loh <i>et al.</i> 2003a). . . . .	9
2.7	Interface slip at the end of the beam (Loh <i>et al.</i> 2003a). . . . .	9
2.8	Profiled sheeting with perfobond ribs (Kim <i>et al.</i> 2010). . . . .	10
2.9	Connection with longitudinal embossed steel plates (Papastergiou <i>et al.</i> 2014). . . . .	10
2.10	Typical cross-sections of composite beam. . . . .	12
2.11	Effective width of concrete compression flange at a composite beam cross-section (EN 1994-1-1 2004). . . . .	13
2.12	Plastic stress distributions for a composite beam under sagging bending for full shear connection. . . . .	13
2.13	Plastic stress distribution for a composite beam under sagging bending for partial shear connection. . . . .	13
2.14	Beam with partial composite action: (left) force and deformation of steel beam and concrete slab; (right) stress distribution along section height (Li <i>et al.</i> 2007). . . . .	14
2.15	Beam with full composite action: (left) force and deformation of steel beam and concrete slab; (right) stress distribution along section height (Li <i>et al.</i> 2007). . . . .	14
2.16	Beam without composite action: (left) force and deformation of steel beam and concrete slab; (right) stress distribution along section height (Li <i>et al.</i> 2007). . . . .	14
2.17	Headed stud (Johnson 2004). . . . .	15
2.18	Channel connectors (Johnson 2004). . . . .	15
2.19	Bar connectors (Johnson 2004). . . . .	15
3.1	Cross-section and loading - specimen SCB-1 (Nie and Cai 2003). . . . .	18
3.2	Cross-section and loading - specimen SCB-3 (Nie and Cai 2003). . . . .	18
3.3	Cross-section and loading - specimen E1 (Chapman <i>et al.</i> 1964). . . . .	18
3.4	A typical composite beam with beam and shell finite elements. . . . .	19
3.5	A typical composite beam FE mesh. . . . .	19
3.6	Stress-strain relationship for concrete - specimen E1 (Chapman <i>et al.</i> 1964). . . . .	21
3.7	Stress-strain relationship for reinforcing steel. . . . .	21
3.8	Stress-strain relationship for concrete - specimens SCB-1 and SCB-3 (Nie and Cai 2003). . . . .	22
3.9	Stress-strain relationship for structural steel - specimen E1 (Chapman <i>et al.</i> 1964). . . . .	23
3.10	Assumption 1: Equivalent section (Chapman <i>et al.</i> 1964). . . . .	23
3.11	Assumption 2: Equivalent stress-strain relationship for structural steel (Chapman <i>et al.</i> 1964). . . . .	24
3.12	A typical shear connectors constitutive law in terms of force and displacement. . . . .	25

## List of Figures

---

3.13	Specimen E1: Load vs. mid-span deflection (Chapman <i>et al.</i> 1964). . . . .	26
3.14	Specimen E1: Load vs. mid-span deflection - different procedures. . . . .	26
3.15	Specimen E1: Load vs. mid-span deflection - level of shear connection: 136%. . . . .	27
3.16	Specimen E1: Load vs. mid-span deflection - level of shear connection: 130%. . . . .	27
3.17	Specimen E1: Load vs. mid-span deflection - level of shear connection: 118%. . . . .	27
3.18	Specimen E1: Load vs. mid-span deflection - level of shear connection: 100%. . . . .	27
3.19	Specimen E1: Load vs. mid-span deflection - level of shear connection: 89%. . . . .	27
3.20	Specimen E1: Load vs. mid-span deflection - level of shear connection: 71%. . . . .	27
3.21	Specimen E1: Load vs. mid-span deflection - level of shear connection: 47%. . . . .	28
3.22	Specimen E1: Load vs. mid-span deflection - all levels of shear connection. . . . .	28
3.23	Specimen SCB-1: Bending moment vs. mid-span deflection (Nie and Cai 2003). . . . .	29
3.24	Specimen SCB-1: Bending moment vs. mid-span deflection - different procedures. . . . .	29
3.25	Specimen SCB-3: Bending moment vs. mid-span deflection (Nie and Cai 2003). . . . .	29
3.26	Specimen SCB-3: Bending moment vs. mid-span deflection - different procedures. . . . .	29
3.27	Specimen SCB-1: Bending moment vs. mid-span deflection - all levels of shear connection. . . . .	30
3.28	Specimen SCB-3: Bending moment vs. mid-span deflection - all levels of shear connection. . . . .	30
4.1	Load vs. mid-span deflection - for different concrete slab strengths. . . . .	36
4.2	Load vs. mid-span deflection - for different concrete slab effective widths. . . . .	37
4.3	Mesh size 15. . . . .	38
4.4	Mesh size 30. . . . .	38
4.5	Mesh size 45. . . . .	38
4.6	Mesh size 90. . . . .	38
4.7	Mesh-sensitivity analysis of specimen E1 (Chapman <i>et al.</i> 1964). . . . .	38
4.8	Proposed procedure E1. . . . .	39
4.9	Proposed procedure E1-sc. . . . .	39
4.10	Proposed procedure E1-cc. . . . .	39
4.11	Reinforcement embedded in concrete slab. . . . .	40
4.12	Load vs. mid-span deflection - different proposed procedures. . . . .	40
4.13	The fracture energy cracking criterion: (left) displacement; (right) energy. . . . .	41
4.14	Load vs. mid-span deflection - fracture energy cracking criterion: displacement. . . . .	42
4.15	Load vs. mid-span deflection - fracture energy cracking criterion: energy. . . . .	42
4.16	Load vs. mid-span deflection, all tension stiffening methods - beam E1-sc. . . . .	43
4.17	Load vs. mid-span deflection, all tension stiffening methods - beam E1-cc. . . . .	43

# List of Tables

3.1	Parameters of specimens. . . . .	17
3.2	Properties of the structural steel (Chapman <i>et al.</i> 1964). . . . .	22
3.3	Level of shear connection of specimen E1. . . . .	27
3.4	Level of shear connection of specimens SCB-1 and SCB-3. . . . .	29
4.1	Differences between design codes. . . . .	35
4.2	Influence of the slab concrete strength on the composite beam. . . . .	36
4.3	Influence of the slab concrete width on the composite beam. . . . .	37
4.4	Differences between the proposed procedures. . . . .	40
4.5	Number of finite elements for each proposed model. . . . .	43



# Chapter 1

## Introduction

### 1.1 General aspects

The steel-concrete composite beams have seen widespread use both in modern buildings and highway bridges in recent decades due to multiple advantages that occur by combining the individual mechanical properties of the component materials, concrete and steel.

The composite beam consists of a steel beam and a portion of concrete slab, connected with shear connectors.

Concrete slab presents high stiffness and robustness in compression where steel is prone to buckling, while the steel presents high strength and ductility in tension where concrete can be easily cracked.

From structural point of view the resulted composite section provides an increase of the rigidity, strength and the ultimate moment capacity of the composite beam, compared with the independent use of each material, and from an economical point of view the resulted composite section presents advantages in terms of saving in steel weight, reduction in the construction depth and shortening the construction period of time.

The composite behavior of concrete slab and steel beam is maintained by the mechanical action of the shear connectors.

The behavior of the composite connection depends on many factors, such as strength and dimension of shear connectors, spacing between shear connectors and concrete strength.

A fundamental aspect in composite structures is the level of connection and interaction between the components.

The term *full shear connection* relates to the case in which the connection between the components is able to fully resist the forces applied. This is the most common situation. However, over the last decades the use of composite beams in construction has led to many instances when the connection cannot resist all the forces applied. This situation is named *partial shear connection*. In this case, the failure due to longitudinal shear forces may occur before either of the other components of the composite beam reaches its own failure state.

When it comes to serviceability limit state (SLS) of composite beams, the condition when the connection between the components of the beam is considered as infinitely stiff is said to consist of *full interaction*. This can be achieved in design but in practice is impossible, due to the limitation of

the number of shear connectors that the top flange can accommodate or many other reasons, and the situation when the connection is more limited in terms of stiffness - *partial interaction* needs to be considered.

Generally, the situations mentioned above are presented in design codes of each country, such as EN 1994-1-1 2004, AS-2327.1 2003, AISC-LRFD 1994.

With the development of computational tools and computers, today's researchers commonly use more complicated analysis such as finite element models to analyze the structural systems, in order to find out more about the behavior of composite beams (Bursi, Sun, *et al.* 2005, Queiroz *et al.* 2007, Nie, Tao, *et al.* 2011, Chiorean 2013, among many others).

The *finite element method* (FEM) acts as a link between the experimental tests and the mechanical and analytical modeling.

When using FEM on composite beams, a particular difficulty represents modeling the behavior of reinforced concrete and the interaction between the concrete slab and structural steel. Despite this, FEM permits a better understanding of the experimental behavior and the simplified methods.

## 1.2 Objectives

The main objective of this thesis is to present an efficient procedure, for nonlinear inelastic analysis of three-dimensional composite steel-concrete beams. The proposed procedure accounts for material nonlinear constitutive equations.

The overall aim of the paper is to investigate and improve the understanding of the behavior of steel-concrete composite beams, considering full and partial shear connection.

The specific objectives of this study are focused on the structural behavior of composite beams by means of the analysis of the results related to:

- Finite element method
- Load - displacement analysis
- Differences between design codes
- Influence of the slab concrete strength
- Influence of the slab concrete width
- Mesh-sensitivity analyzes
- Fracture energy effects

The axiomatic idea behind the study is that the reported results demonstrate that the numerical approach is a valid tool for extensive parametric studies on composite beams with full and partial shear connection.



### 1.3 Structure and contents of the thesis

The present study is organized in five Chapters, as follows:

*Chapter 1 - Introduction* - presents the general aspects regarding this study: a short introduction about composite beams, objectives and significance of the research.

*Chapter 2 - State of the art review* - highlights the present knowledge in steel-concrete composite beams with full and partial shear connection. A discussion is made upon several experimental programs carried out by different researchers, across the world and other analytically studies. Also, prescriptions of design codes are presented.

*Chapter 3 - Finite element model* - describes the proposed procedure. The results are validated by comparison against experimental tests, as well as against alternative numerical studies.

*Chapter 4 - Parametric studies* - comprises the methodology presented by different design codes in order to attain full shear connection, the influence of the concrete slab strength and the effective width of concrete slab on the structure behavior in steel-concrete composite beams, the mesh-sensitivity analysis and the fracture energy effects on the structural response of composite beams.

*Chapter 5 - Conclusions and future lines of investigations* - the final chapter presents a synthetic view of the proposed procedure and of the parametric studies. Some suggestions are being made about future research issues.

*Bibliography*



# Chapter 2

## State of the art review

### 2.1 Introduction

The subject of steel-concrete composite structures is of high interest since 1950s. Since then, numerous experimental programs have been carried. In all this time analytical and numerical procedures were developed and improved, based on experimentally obtained results, which are always considered as a reference - true values. Also, the design codes became richer in prescriptions and suggestions. Therefore, the subject shows great importance and is still an active field of research.

### 2.2 Experimental results

One of the first tests was made of by Culver *et al.* 1961. The specimens were simply supported, as presented in Fig. 2.1. The connection between the concrete slab and structural steel was achieved by means of shear studs. Deflection, end slip and strain readings were taken during the test. One of several conclusions revealed by the experimental program was that large values of slip between concrete slab and steel beam do not significantly alter the ultimate moment or the load deflection characteristics of the composite section.

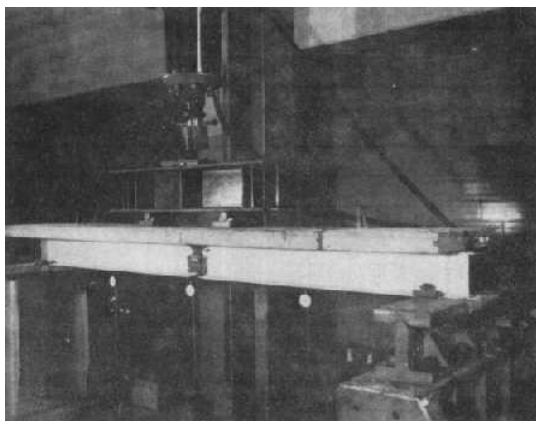


Figure 2.1: Test setup (Culver *et al.* 1961).

Although, many effects of the composite beams remained unknown, such as the distribution and spacing of shear studs along the beam and the interaction created by bond and friction.

These were partially solved through the study of Slutter and Driscoll Jr 1963, who concentrated his work on flexural strength of steel and concrete composite beams. In the experimental program twelve single-span composite beams and one two-span continuous beam were tested.

The steel-concrete composite beams with a single-span made the subject of several studies.

The influence of the presence of shear connectors was investigated in order to determine the flexural strength. In this sense, steel-concrete composite beams with and without connectors were tested.

In the case of the beams without shear connectors, the shear connection consisted only of the natural bond between the two materials were tested. The results showed that the failure was caused by shrinkage of the concrete and the only shear force acting was due to friction caused by loads on the top flange. Different testing procedures were applied. In one case, loads were suspended from the steel beam and only the dead weight of the concrete was available to produce frictional shear forces along the top flange of the steel beam. Complete separation except at the ends of the member took place at a relatively low load. In the other case the test load was applied on top of the member and larger frictional forces were developed.

In the case of the beams with shear connectors, the shear connection consisted of mechanical shear connectors welded to the top flange of the steel beams, which were of several types: "L" shaped bent studs, channel connectors and headed studs. The connectors were arranged on two and three rows. These beams were divided into two categories, which are named adequate and inadequate by Slutter and Driscoll Jr 1963. The former is achieved when the sum of the ultimate strengths of shear connectors in the shear span is equal to or greater than the maximum compressive force in the slab at the section of maximum moment, and the latter when the sum of the ultimate strengths of the shear connector is less than the maximum compressive force in the slab. Therefore, no calculation for determining the weakest component of the composite section has been made and the concrete was assumed to be. In the case of the beams with the number of connectors less than the required number in order to obtain the maximum flexural strength was remarked that failure occurred only after the maximum strength in connectors was achieved. This represents a strong relationship between the ultimate strength of shear connectors and the ultimate flexural capacity of the composite beam.

The spacing of the connectors was also part of the study. The composite beams were subjected to concentrated loads (i.e. four point bending) and uniformly distributed load, a situation that has been achieved by placing the concentrated loads at close range. It was noticed that uniform spacing of shear connectors is satisfactory for beams supporting a uniform load.

The steel-concrete composite beams with two-span were tested first by loading only one span at a time and stopping the loading below ultimate as in the simple beam tests. Finally the members were tested to failure with two concentrated loads on each span. It was observed during the tests that wide cracks formed in the negative moment region even at loads below working load and it was suggested that controlling of the cracks should be employed in the design, either in the form of an expansion joint or sufficient slab reinforcement to distribute cracks along the member.

One of the largest experiments on simply supported beams, often used as benchmark tests by numerous researchers was conducted by Chapman *et al.* 1964.

The researched focused on seventeen simply supported composite beams subjected to static concentrated and to distributed loading applied on the axis of the beam, as presented in Fig. 2.2. All the beams present overhanging regions, but according to Chapman *et al.* 1964, a more rational test procedure would have been to limit the slab length to the distance between supports. The width of the concrete slab was chosen to enable full plasticity in the steel beam. The connection between the concrete slab and steel beam was achieved through welded stud shear connectors. Several push-out tests were carried out on the types of connector employed in the beams, in order to correlate the push-out and composite beam results. The number of the connectors varied within the range which might be contemplated for design purposes.

Considerable axial forces were noticed in shear connectors; to develop these force the connectors must be properly anchored within the compression zone of the slab. The effect of interface slip was observed. The composite beams were calculated after a simple rectangular stress distribution, but the failure occurred at a load exceeding the calculated value. This proves the reliability of simple rectangular stress distribution for ultimate moments. The mode of failure was due to the crushing of the slab and stud failure, with the mention that the latter occurred only in those beams where the connection was designed to fail when the beam reaches its nominal ultimate moment.

An equal spacing of the connectors in the case of uniformly distributed load was recommended; also the same was suggested by Slutter and Driscoll Jr 1963.

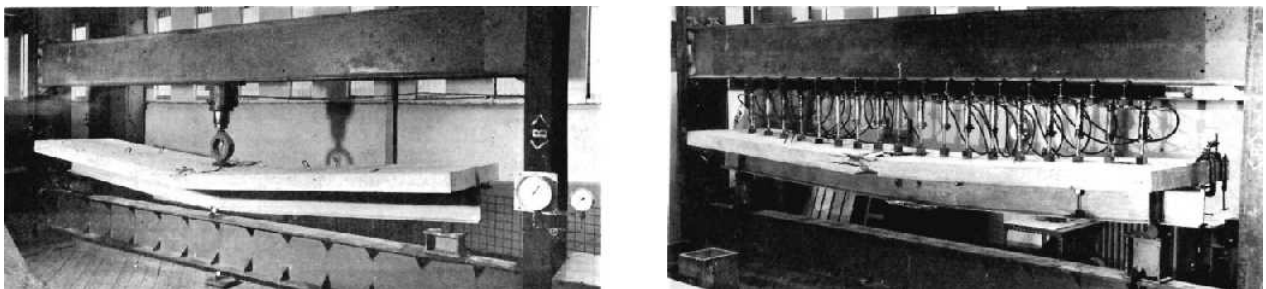


Figure 2.2: Test setup (Chapman *et al.* 1964).

Ansourian 1981 conducted an experimental program on six continuous composite beams consisting of structural steel beams connected to concrete slabs with welded studs through which the composite action was achieved. The beams were subjected to concentrated loading.

One out of many conclusions of the study, revealed that the rotation capacity of sagging moment hinges under concentrated loading is influenced by the cross-section dimensions, yield stress and concrete strength.

An investigation of the seismic performance of composite moment resisting frames with full and partial shear connection subjected to seismic loading was developed by Bursi and Gramola 2000. For this purpose six full scaled specimens were subjected to horizontal displacements in a quasi-static cyclic and pseudo-dynamic regime.

The results demonstrate that the behavior of the composite beams with partial shear connection is satisfactory in terms of yielding and of maximum strength capacity as well as of ultimate displacement ductility similar to the companion full shear connection beams. A similar behavior can be expected under severe earthquakes. Moreover, predictions based on code provisions overestimate the actual

strength capacity of composite beams and, thereby, appear to be unsafe in the presence of large hysteretic displacements controlling the structural response. According to Bursi and Gramola 2000, these inaccuracies combined with lack of information on section and member ductility may represent a major obstacle in the widespread use of composite systems in seismic zones.

The shear slip effects on composite beams were investigated in detail in the experimental program conducted by Nie and Cai 2003. Six specimens were tested, four simply supported and two continuous steel-concrete composite beams. Half of the simply supported specimens were subjected to one-point loading and the other half to two-point loading. The continuous beams were two-span specimens. The spans were equal and one concentrated load was applied at the center of each span. The shear stud distribution was in accordance with the shear diagram. The continuous beams measurements of slip distribution under different loading along the span showed a strong relationship between load and slip.

According to the experimental results obtained (Nie and Cai 2003), it was suggested that a linear behavior can be assumed when the ratio between the applied load and ultimate load capacity is less than 0.6. If the load is increased the relationship becomes highly nonlinear. The maximum slips were observed near the ends of beam. Comparing the measured slip obtained by the specimens with different shear distribution it is remarked that pitches of the shear studs have significant effects on the slip.

In order to investigate the steel-concrete composite beams behavior subjected to hogging moment, an extensive experimental program has been conducted by Loh *et al.* 2003a. The specimens presented a composite slab, with profiled steel sheeting. The program consisted of eight specimens, which were tested with different levels of shear connection and reinforcement ratio. The beams were tested upside down and the force is applied gravitational on the structural steel, as show in Fig. 2.3. According to Loh *et al.* 2003b and Loh *et al.* 2004, two types of loading pattern were employed, static loading until failure for three beams and quasi-static loading before testing to failure for the remaining five beams.

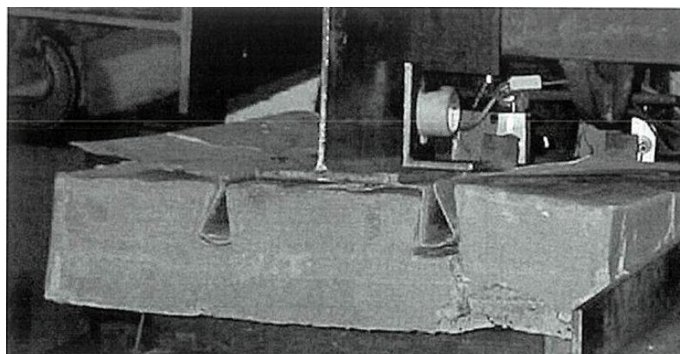


Figure 2.3: Test setup (Loh *et al.* 2003a).

The local buckling of the steel beam flange and web, as presented in Fig. 2.4, and the fracture of the shear connectors, as presented in Fig. 2.5, were the two failure modes observed. The former was developed in the beams with a higher degree of shear connection and higher amount of reinforcement. The latter was present especially in beams with less than 50% of full shear connection and was accompanied by crushing of the concrete slab at the interface and buckling of the profiled steel sheeting at mid-span (Fig. 2.6). Before the failure of connectors occurred, a significant interface

slip was noticed at the ends of the beam (Fig. 2.7).

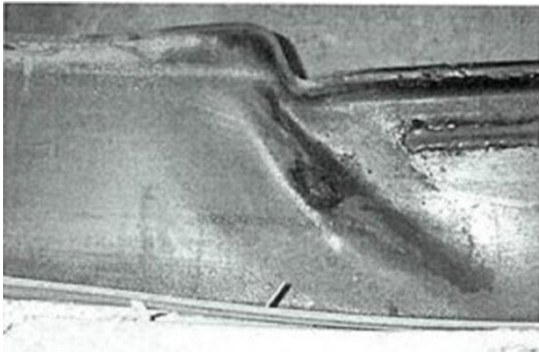


Figure 2.4: Web and flange buckling (Loh *et al.* 2003a).

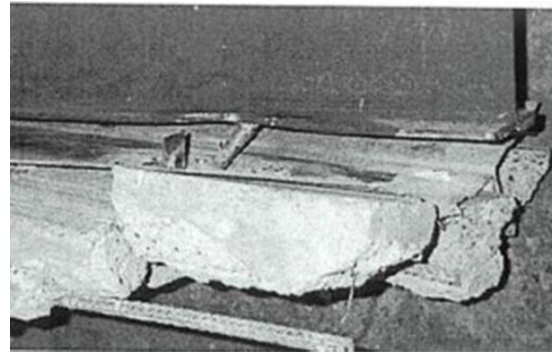


Figure 2.5: Failure of stud connector (Loh *et al.* 2003a).

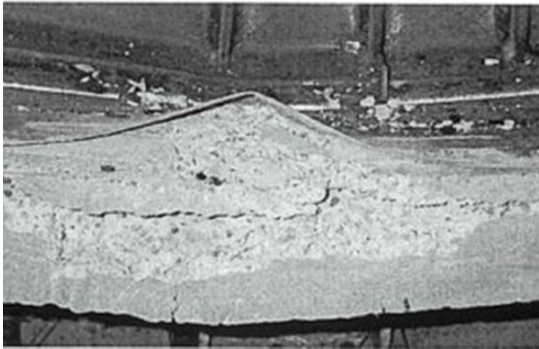


Figure 2.6: Concrete crushing and profiled steel sheeting buckling at mid-span (Loh *et al.* 2003a).



Figure 2.7: Interface slip at the end of the beam (Loh *et al.* 2003a).

An experimental program concerning the evaluation of effective width in steel-concrete composite beams was conducted by Amadio, Fedrigo, *et al.* 2004. The study is performed on four specimens subjected to sagging and hogging bending moments.

It was concluded that in the presence of hogging moment the shear-lag phenomenon becomes less important when the beam approaches the collapse condition and of sagging bending moment the effective width evaluated through the stress distribution in the concrete slab remarkably varies with the load level, approaching the whole slab width at collapse. Also, some suggestions in order to improve EN 1994-1-1 2004 design codes were made.

The simply supported prestressed steel-concrete composite beams behavior was studied by Nie, Cai, *et al.* 2007 through experimental and analytical studies. Eight specimens were tested in the experimental program. Both cast-in-place slab and slab consisting of precast panel and cast-in-place concrete were included in the testing.

The results concluded that the yield moment, ultimate moment and elastic stiffness are increased by the prestressing force and that a more accurate calculation of the yield moments of prestressed steel-concrete composite beams is achieved by accounting the slip effect and the tendon force.

In the last few years, the subject of steel-concrete composite beams has known a great development. A series of new innovative solutions were proposed.

Feldmann *et al.* 2008 and Rauscher *et al.* 2008 proposed steel dowels created on the steel web by cutting a steel profile. A connection with perfobond ribs, as depicted in Fig. 2.8, was developed by Kim *et al.* 2010, which presents the advantage that allows for prefabrication without supplementary

cast in place concrete for the deck.

In order to avoid concreting the openings of the slab elements in which shear studs are enclosed, which is the traditional solution to apply the composite action in a steel-concrete composite bridge with prefabricated slab elements and to reduce the overall construction time, Papastergiou *et al.* 2014 proposed a new type of connection for steel-concrete composite beams under static and fatigue loading. The connection involves replacing the shear studs in favor of a pair of longitudinal embossed steel plates on it, as presented in Fig. 2.9.

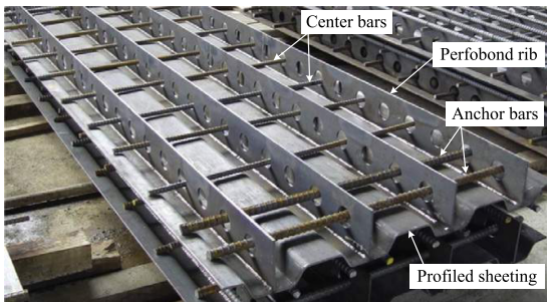


Figure 2.8: Profiled sheeting with perfobond ribs (Kim *et al.* 2010).



Figure 2.9: Connection with longitudinal embossed steel plates (Papastergiou *et al.* 2014).

These experiments, among others, on steel-concrete composite beams, resulted in a need to investigate the behavior of shear connection. Many researchers considered that there is an absence of an experimental data. Consequently, numerous experimental programs were carried out on shear studs, such as Slutter and Fisher 1966, Ollgaard *et al.* 1971, Gattesco and Giuriani 1996, Lam *et al.* 2005.

### 2.3 Numerical results

A significant number of numerical and analytical procedures were developed in the last few decades from the simplest to the most complex. Mostly this was due to strong development of computer industry, which produces tools with an increasing computational power. Accordingly, most of the research on steel-concrete composite beams has been focused on the development of specific finite elements with either displacement, force-based or mixed formulations.

Three-dimensional analysis with solid elements is obviously the procedure which will produce the most accurate results and be able to simulate the complex phenomena. Nonetheless, when dealing with practical engineering problems, three-dimensional analysis often becomes too expensive and sometimes unavailable. Problems, such as mesh generation, can become difficult to solve. Although, this type of analysis is widely used among researchers, such as El-Lobody *et al.* 2009 and Vasdravellis *et al.* 2012, who chose to model both the structural steel and concrete slab with solid elements.

In order to reduce the computational effort without modifying the results, some authors use shell and solid finite element type for structural steel and concrete, respectively (Queiroz *et al.* 2007).

Many researchers have carried out numerical and experimental investigations of the behavior of composite girders such as those published by Baskar *et al.* 2002, Oehlers *et al.* 1997, Nie and Cai



2003, Nie, Cai, *et al.* 2007, Zona *et al.* 2011, Nie, Tao, *et al.* 2011.

An interesting approach was developed by Chiorean 2013 who proposed an efficient computer method for nonlinear inelastic analysis of three-dimensional steel-concrete composite beams with partial shear connection, using only one element per physical member. The model accounts for material inelasticity, gradual yielding and is described through basic equilibrium, compatibility and material nonlinear constitutive equations. The proposed nonlinear analysis formulation was implemented in a general nonlinear static purpose computer program, *Nefcad*. The effectiveness of the proposed method and the reliability of the code were validated by comparing the predicted results by *Nefcad* with those given by Abaqus software package (Abaqus 2011). Also, the computer program was used by other authors (Buru *et al.* 2014) who demonstrated its reliability.

Similar approach was developed by Nguyen *et al.* 2009 who proposed a numerical model based on a nonlinear two-field mixed finite element formulation for predicting the behavior of continuous composite beams with discrete shear connectors has been presented.

Many researchers concluded that a very important aspect in the design of composite beams is the design of shear connection. Therefore, several numerical procedures were developed, such as Slutter and Fisher 1965, Mistakidis *et al.* 1994 etc. A three-dimensional bar element was developed by Razaqpur *et al.* 1989 which can be used to model the nonlinear behavior of the shear connectors in composite steel-concrete structures, taking into consideration both the shear and tension effects (uplift effect). Also, procedures on finite element method were carried out. The research of Lam *et al.* 2001, using this numerical procedure, accurately predicts the load-slip characteristics of the stud, the shear connection capacity and the failure modes. The procedure has been extended by Lam *et al.* 2011 to simulate the behavior of headed stud shear connectors with precast hollow core slabs.

The main aspects that deserve an increased attention when modeling steel concrete composite beam, in order to obtain desired values by avoiding the convergence problems, are the presence of concrete, which increases inevitably the complexity of analysis, the connection between the steel and concrete.

## 2.4 Design prescriptions

Generally, the aim of the design codes is to help the engineer to design structural elements that have adequate strength, are serviceable, stable, durable and fire-resistant, if required, and satisfies other objectives such as economy and ease of construction.

A composite member is a structural member with components of concrete and of structural or cold-formed steel, interconnected by shear connection so as to limit the longitudinal slip between concrete and steel and the separation of one component from the other.

In the case of composite beams, which are composite members subjected mainly to bending, the section is composed of slab and of structural steel. When the slab includes profiled steel sheets, which are used initially as permanent shuttering and subsequently combine structurally with the hardened concrete and act as tensile reinforcement in the finished floor, it is referred as composite slab. Contrary, it is named concrete slab.

The composite action is achieved through the shear connection, which represents an interconnection between the concrete and steel components of a composite member that has sufficient strength and stiffness to enable the two components to be designed as parts of a single structural member.

The composite behavior occurs only, after the shear connection has become effective due to hardening of concrete, and is achieved through mechanical connectors.

Prior to development of composite action each component shall be designed in accordance to its code (i.e. design code of steel and design code of concrete).

Typical cross-sections of steel-concrete composite beams are presented in Fig. 2.10.

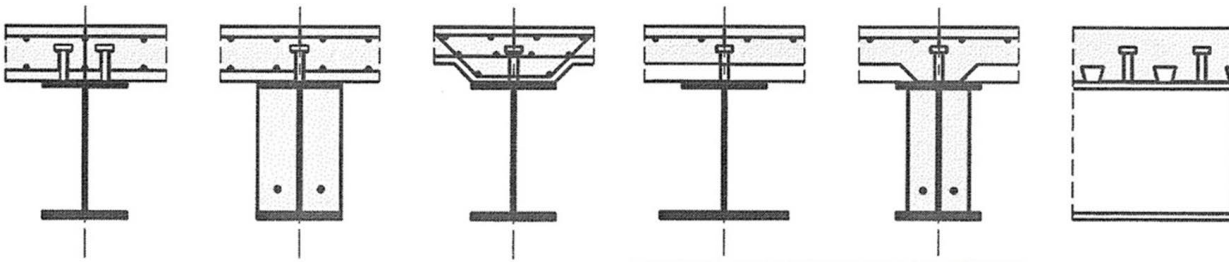


Figure 2.10: Typical cross-sections of composite beam.

The steel-concrete composite cross-section can be classified in four classes, presented in EN 1993-1-1 2005, as follows:

- *Class 1* cross-sections are those which can form a plastic hinge with the rotation capacity required from plastic analysis without reduction of the resistance.
- *Class 2* cross-sections are those which can develop their plastic moment resistance, but have limited rotation capacity because of local buckling.
- *Class 3* cross-sections are those in which the stress in the extreme compression fiber of the steel member assuming an elastic distribution of stresses can reach the yield strength, but local buckling is liable to prevent development of the plastic moment resistance.
- *Class 4* cross-sections are those in which local buckling will occur before the attainment of yield stress in one or more parts of the cross-section.

According to EN 1994-1-1 2004, a composite beam shall be checked for: resistance of critical cross-sections; resistance to lateral - torsional buckling; resistance to shear buckling and transverse forces on webs; resistance to longitudinal shear.

An important variable of the bending resistance of the composite cross-section is the effective width of the concrete slab, which represents the overall width of the portion of a concrete slab, at a composite beam cross-section, considered effective in resisting compression after allowing for shear lag. The width is different, in fact, in elastic and plastic phase, as well as in hogging and sagging bending moment regions.

When elastic analysis is used, current regulations, such as EN 1994-1-1 2004, simplify the problem by assuming a constant effective width over the whole of each span.

Fig. 4.2 presents the equivalent spans, for effective width of concrete flange according to EN 1994-1-1 2004.

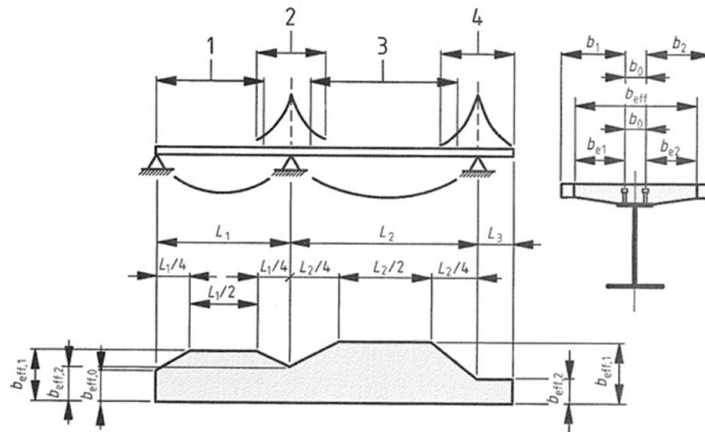


Figure 2.11: Effective width of concrete compression flange at a composite beam cross-section (EN 1994-1-1 2004).

EN 1994-1-1 2004 and AS-2327.1 2003, design codes, suggest that the effective width of the concrete slab on each side of the web should be taken as the effective length span divided by 8,  $L_{ech}/8$ , but not greater than the geometric width,  $b_i$ . EN 1994-1-1 2004 suggests that the geometric width should be taken as the distance from the outstand shear connector to a point mid-way between adjacent webs, whereas AS-2327.1 2003 suggests to take the distance from the center of the web to half of span.

Both the elastic and the plastic theory are applicable on steel-concrete composite beams, but the concepts *full shear connection* (Fig. 2.12) and *partial shear connection* (Fig. 2.13), are applicable only to beams in which plastic theory is used for calculating bending resistances of critical cross-sections. A span of a beam, or a cantilever, has full shear connection when increase in the number of shear connectors would not increase the design bending resistance of the member. Otherwise, the shear connection is partial.

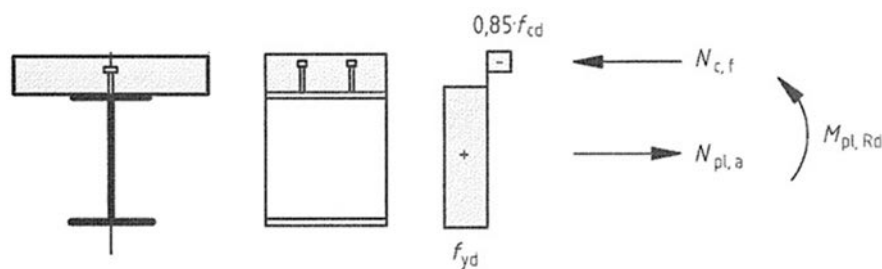


Figure 2.12: Plastic stress distributions for a composite beam under sagging bending for full shear connection.

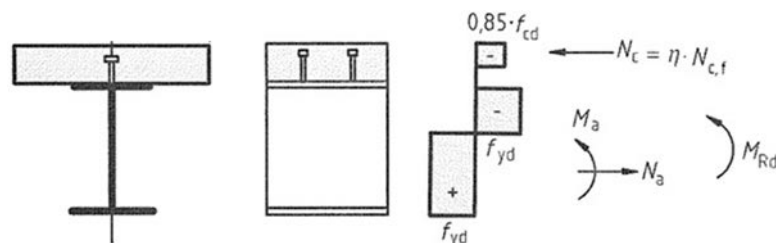


Figure 2.13: Plastic stress distribution for a composite beam under sagging bending for partial shear connection.

## Chapter 2. State of the art review

The distinction between steel-concrete composite beams with partial and full interaction, and without interconnection is shown in Figs. 2.14 to 2.16. It can be noticed that in the case of fully composite beam, which have sufficient shear connectors, the slip is small, whereas in the case of partially composite beams the relative slip is relatively large. In the latter case, only the strength of the structural steel is taken into consideration.

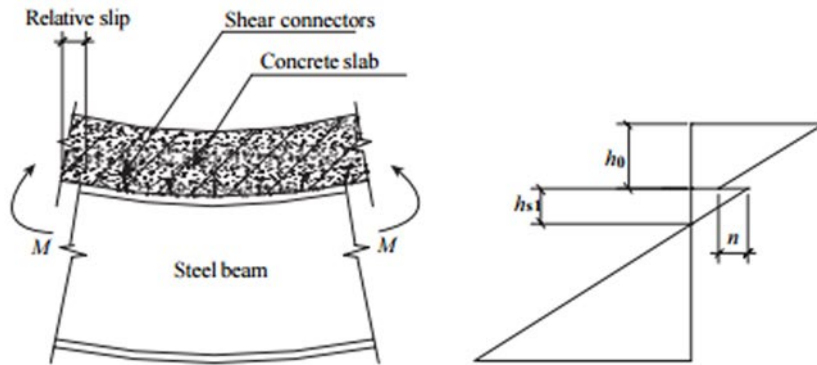


Figure 2.14: Beam with partial composite action: (left) force and deformation of steel beam and concrete slab; (right) stress distribution along section height (Li *et al.* 2007).

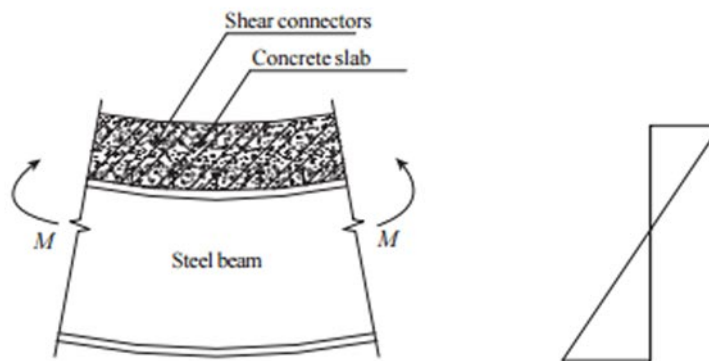


Figure 2.15: Beam with full composite action: (left) force and deformation of steel beam and concrete slab; (right) stress distribution along section height (Li *et al.* 2007).

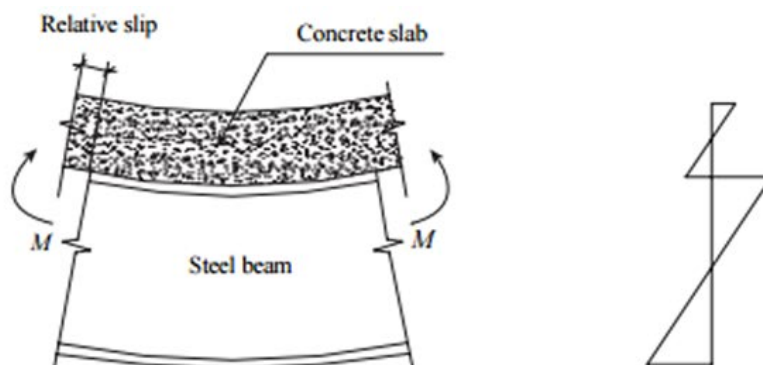


Figure 2.16: Beam without composite action: (left) force and deformation of steel beam and concrete slab; (right) stress distribution along section height (Li *et al.* 2007).

The shear connection between the two components, the concrete slab and the steel beam, can be achieved through different types of mechanical shear connectors, as presented in Figs. 2.17 to 2.19. The most widely used type of connector is the headed stud shear connector (Fig. 2.17).

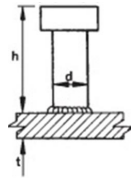


Figure 2.17: Headed stud (Johnson 2004).

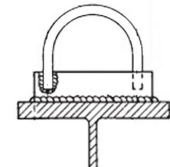
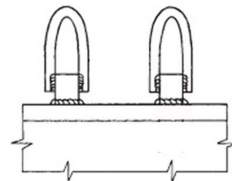
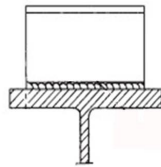
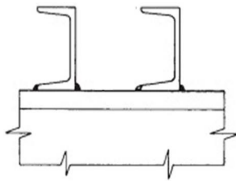


Figure 2.18: Channel connectors (Johnson 2004).

Figure 2.19: Bar connectors (Johnson 2004).

In order to prevent separation of the slab, shear connectors should be designed to resist a nominal ultimate tensile force, perpendicular to the plane of the steel flange, of at least 0.1 times the design ultimate shear resistance of the connectors. In case of using headed stud shear connectors, the most common situation, these should provide sufficient resistance to uplift, unless the shear connection is subjected to direct tension.

Regarding the use of composite beams in building construction EN 1994-1-1 2004 suggests that the number of connectors should be at least equal to the total design shear force for the ultimate limit state divided by the design resistance of a single connector  $P_{Rd}$ , in case of full shear connection and if partial shear connection is desired, it has to be determined by a partial connection theory taking into account the deformation capacity of the shear connectors and the cross-section should be *Class 1* or *Class 2*.

The degree of shear connection, which is defined by the ratio of the number of shear connectors provided within the same length and the number of connectors for full shear connection, is limited in EN 1994-1-1 2004 to a minimum value of 0.4, due to ductility requirements, meanwhile in other design codes, such as AS-2327.1 2003, no limit is imposed.

The shear connectors shall be spaced along the beam so as to transmit longitudinal shear and to prevent separation between the concrete and the steel beam, considering an appropriate distribution of design longitudinal shear force.



# Chapter 3

## Finite element model

### 3.1 Introduction

With the development of high-powered computers, together with finite element software and user friendly graphical interfaces, finite element analysis has become a popular choice for steel-concrete frame structures, even though sometimes the computational efforts may become large. In this study, the advanced numerical simulation is conducted with Abaqus CAE v.6.11 (Abaqus 2011) software, which is one of the most used commercial finite element package for nonlinear analysis of structures.

### 3.2 Geometry of the analyzed structures

#### 3.2.1 General aspects

The present study consists in the analysis of three simply supported beams experimentally tested by other authors, as follows: specimen E1 by Chapman *et al.* 1964 and specimens SCB-1 and SCB-3 by Nie and Cai 2003. The parameters of the experimentally tested specimens are summarized in Tab. 3.1 and the cross-sections and loading in Figs. 3.1 to 3.3

Table 3.1: Parameters of specimens.

		SCB-1	SCB-3	E1
concrete slab	width $b_c$ (mm)	500	800	1219.20
	height $h_c$ (mm)	125	125	152.40
reinforcement	longitudinal - top	7 $\phi$ 6	12 $\phi$ 12	4 $\phi$ 7.90
	- bottom	7 $\phi$ 6	7 $\phi$ 6	4 $\phi$ 7.90
	transversal - top	$\phi$ 6 @ 75	$\phi$ 6 @ 75	$\phi$ 12.7 @ 304.80
	- bottom	$\phi$ 6 @ 75	$\phi$ 6 @ 75	$\phi$ 12.7 @ 152.40
connectors	diameter of shear stud (mm)	19	19	12.70
structural steel	width $b$ (mm)	100	100	152.40
	depth $h$ (mm)	200	200	304.80
	web thickness $t_w$ (mm)	7	7	10.16
	flange thickness $t_f$ (mm)	11.40	11.40	18.20

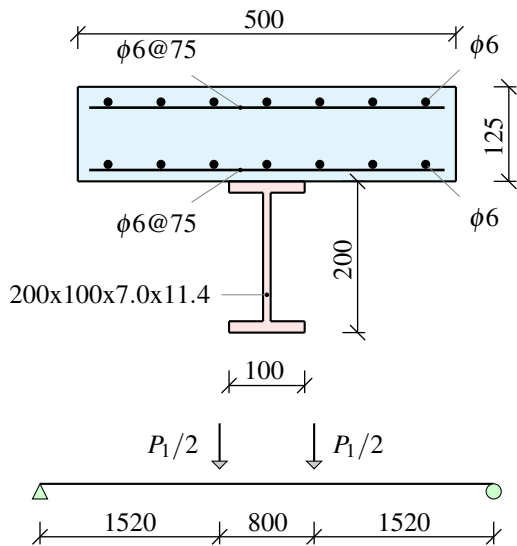


Figure 3.1: Cross-section and loading - specimen SCB-1 (Nie and Cai 2003).

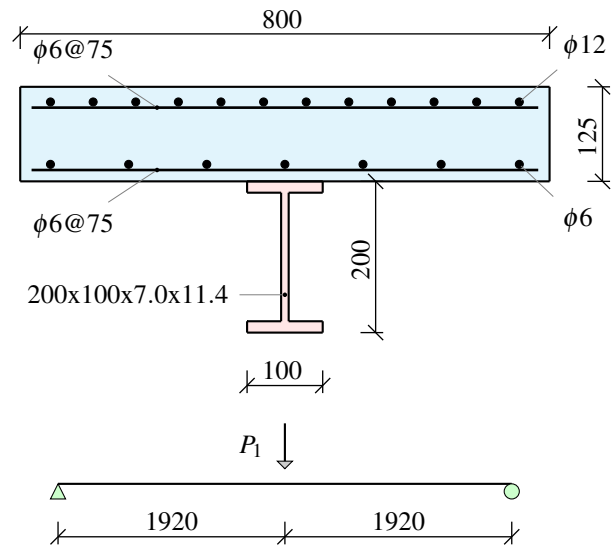


Figure 3.2: Cross-section and loading - specimen SCB-3 (Nie and Cai 2003).

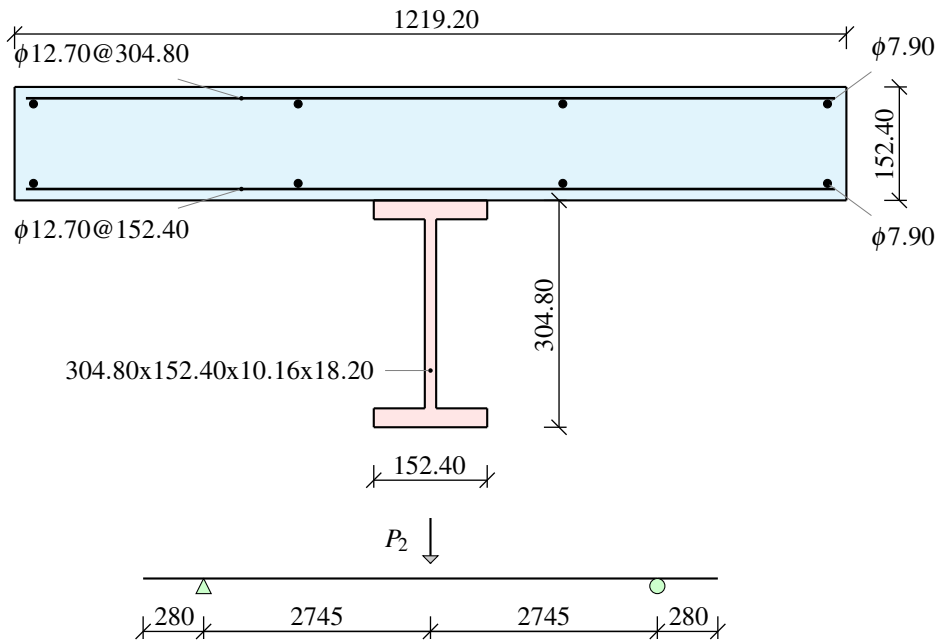


Figure 3.3: Cross-section and loading - specimen E1 (Chapman *et al.* 1964).

### 3.2.2 Element types and mesh construction

The three-dimensional finite element model has the configuration and dimensions of the tested specimens.

The finite element types considered in the model are as follows: S4R element, a 4-node, quadrilateral, shell element with reduced integration and a large-strain formulation for concrete slab, because one dimension, the thickness, is significantly smaller than the other dimensions and this type of element can provide robust and accurate solutions in all loading conditions; B31 element, a one-dimensional line element in three-dimensional space, that has stiffness associated with deformation (axial shortening/elongation, curvature change - bending and torsion) of the line, the beam's axis, for steel section. A typical composite beam with shell finite element for the concrete slab and beam finite



element for the structural steel is shown in Fig. 3.4.

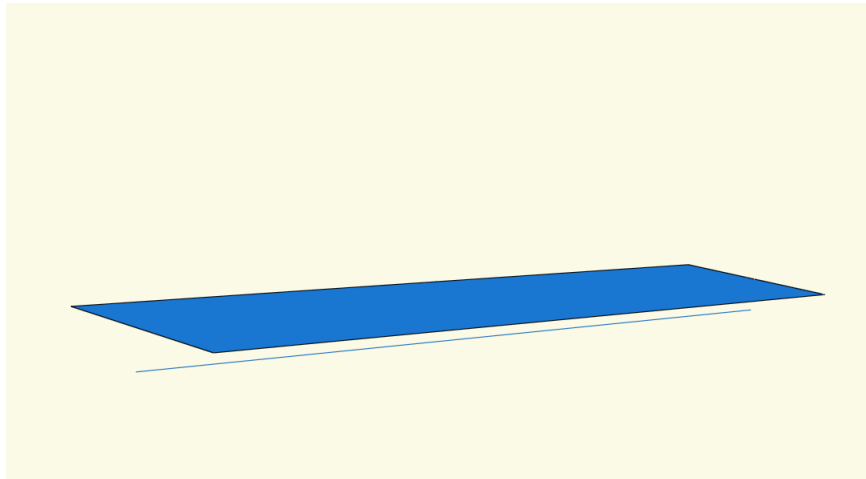


Figure 3.4: A typical composite beam with beam and shell finite elements.

Abaqus presents the option of modeling the reinforcement as distributed or spread over the shell using the *rebar layers* option, which means that the reinforcement is another shell with a cross-section equivalent to the steel rebars it represents. Although, this method does not allow us to model changes in the spacing and geometry of the rebars, it is used in the present study and other studies done by other authors, such as Amadio and Fragiacommo 2003 and Bursi, Sun, *et al.* 2005.

The connection between the concrete slab and steel beam is achieved by means of connector elements, CONN3D2, available in the software library. Each connector element has two basic connection components, one translational type - *cartesian* and one rotational type - *align*. For the two in-plane translational directions the relative behavior is defined by a constitutive law in terms of force and displacement which is experimentally obtained from push-out tests on shear studs. In the absence of experimental data it can be described using the relation proposed by Ollgaard *et al.* 1971.

The investigations on the mesh dimension indicate that the optimized mesh has an aspect ratio of elements close to 1:1; an average size of 45 mm for beam E1 and 40 mm for beam SCB-1 and SCB-3 provides accurate results. A typical finite element mesh for a composite beam is shown in Fig. 3.5.

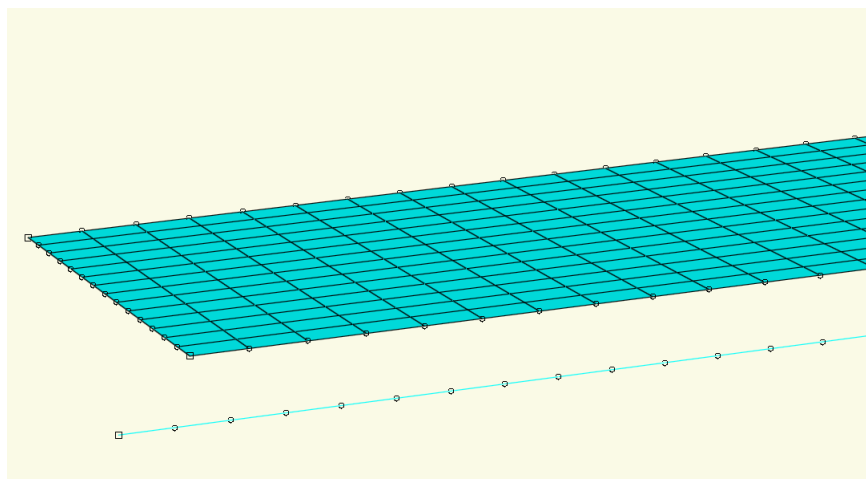


Figure 3.5: A typical composite beam FE mesh.

## 3.3 Material modeling

### 3.3.1 Concrete and reinforcing steel

When modeling composite structures with finite elements, the main difficulty appears at the time of introducing the reinforced concrete. The Abaqus software package provides various forms of modeling it. In the present study the concrete model chosen is *concrete damaged plasticity*, which allows us to introduce both behaviors of the concrete in compression and tension, respectively.

When the concrete is loaded in compression, the initial response is linear. As the stress increases, inelastic deformations appear. When ultimate stress is reached, the material loses strength until it can no longer carry any stress. If the load is removed, the inelastic strain remains.

The main trait of the concrete behavior is to be considered independent from the reinforcement. The effects that appear at the reinforcement - concrete interface (e.g. bonding, slip, cracks) can be approximately modeled introducing tension stiffening in the concrete model that simulates transferring the load between cracks through the reinforcement. This problem was noticed and mentioned by other authors, such as Gil *et al.* 2008.

Further on the analyzed specimens are described separately due to the differences that occur.

#### 3.3.1.1 Specimen E1, tested by Chapman *et al.* 1964

The constitutive relation for concrete under compression is represented by a second-degree parabola, which is achieved by introducing the experimental results (Chapman *et al.* 1964) in expression Eq. 3.1, provided by EN 1992-1-1 2004 for short term uniaxial loading, as depicted in Fig. 3.6. The characteristic compressive cylinder strength of concrete,  $f_{ck}$ , is taken as  $32.68 \text{ N/mm}^2$ . The mean value of concrete cylinder compressive strength and the modulus of elasticity are obtained as  $f_{cm} = f_{ck} + 8 \text{ N/mm}^2$  and  $E_{cm} = 9500f_{cm}^{1/3}$ .

$$\sigma_c = f_{cm} \frac{k\eta - \eta^2}{1 + (k-2)\eta} \quad (3.1)$$

where:  $\eta = \frac{\varepsilon_c}{\varepsilon_{c1}}$  and  $k = 1.05E_{cm} \frac{|\varepsilon_{c1}|}{f_{cm}}$ .

The values of compressive strain at the peak stress  $\varepsilon_{c1}$ , ultimate compressive strain  $\varepsilon_{cu1}$  and Poisson ratio  $\nu$  are selected as 0.0020, 0.0035 and 0.2, respectively.

The model to account for axial tensile strength of concrete (Eq. 3.2) is taken into account in the present investigation, as shown in Fig. 3.6. The peak stress is obtained as  $f_{ctm} = 0.3f_{ck}^{2/3}$  and the tensile elastic modulus before cracking  $E_t$  is assumed the same as compressive elastic modulus  $E_{cm}$ .

$$\sigma_t = f_{ctm} \left( \frac{\varepsilon_{el}}{\varepsilon_t} \right)^{0.4} \quad (3.2)$$

The reinforcing steel is modeled as an elasto-plastic material with a strain hardening and yielding plateau beyond the elastic phase as shown in Fig. 3.7. It is assigned a three-linear stress-strain law,

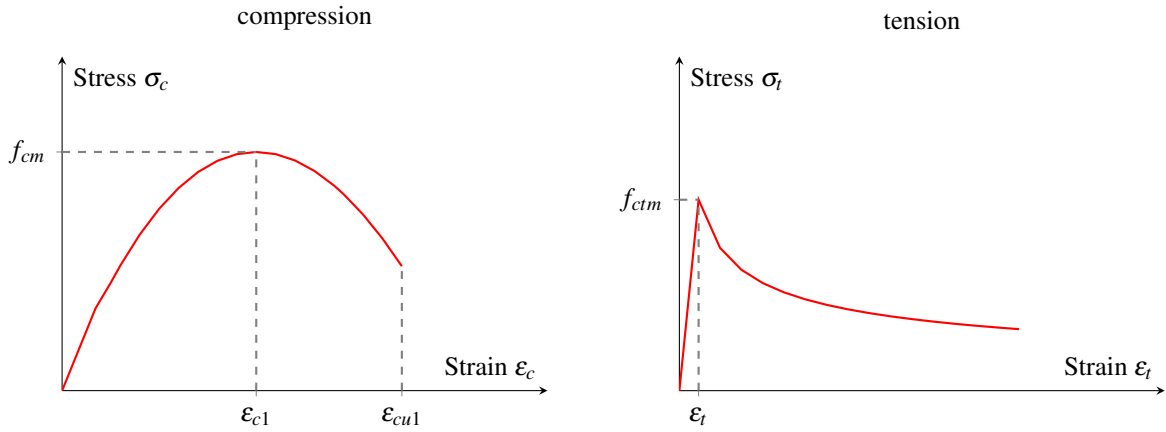


Figure 3.6: Stress-strain relationship for concrete - specimen E1 (Chapman *et al.* 1964).

symmetrical in tension and compression.

The values of yield strength  $f_y$ , Young's modulus  $E_s$ , strain hardening modulus  $E_{sh}$ , strain at the beginning of the strain hardening  $\epsilon_{sh}$  and the Poisson's ratio  $\nu$  are  $320 \text{ N/mm}^2$ ,  $205000 \text{ N/mm}^2$ ,  $1000 \text{ N/mm}^2$ ,  $0.02$  and  $0.3$ , respectively.

The strain hardening part is defined by Eq. 3.3:

$$\sigma_h = f_y + (\epsilon_{sy} - \epsilon_{sh}) E_{sh} \quad (3.3)$$

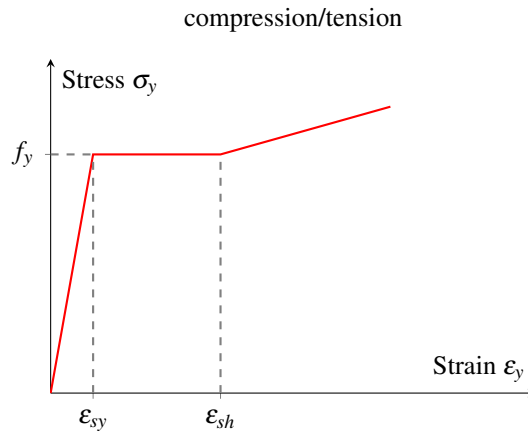


Figure 3.7: Stress-strain relationship for reinforcing steel.

### 3.3.1.2 Specimens SCB-1 and SCB-3, tested by Nie and Cai 2003

The constitutive relation for concrete under compression is represented by the modified model of Hognestad 1951, which is a combination of a second-degree parabola - for ascending part (Eq. 3.4a), and a straight line - for descending part (Eq. 3.4b). The curve is depicted in Fig. 3.8:

$$\sigma_c = f_c \left[ 2 \frac{\epsilon}{\epsilon_{c0}} - \left( \frac{\epsilon}{\epsilon_{c0}} \right)^2 \right] \quad (3.4a)$$

$$\sigma_c = f_c \left[ 1 - \gamma \left( \frac{\epsilon - \epsilon_{c0}}{\epsilon_{cu} - \epsilon_{c0}} \right) \right] \quad (3.4b)$$

where:  $f_c$  and  $\gamma$  represent the cylinder compressive strength and the degree of strain-softening in the concrete (i.e. 0.15), respectively. The cylinder compressive strength  $f_c$  is obtained as  $0.80f_{cu}$ , and  $f_{cu}$  represents the cubic compressive strength and is taken as  $27.70 N/mm^2$  (Nie, Tao, *et al.* 2011).

The values of compressive strain at the peak stress  $\epsilon_{c0}$ , ultimate compressive strain  $\epsilon_{cu}$  and Poisson ratio  $\nu$  are selected as 0.0020, 0.0035 and 0.2, respectively.

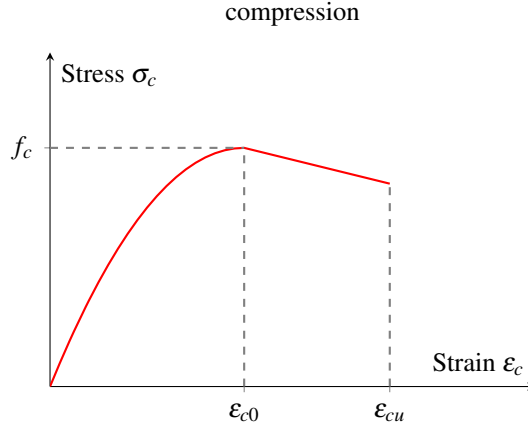


Figure 3.8: Stress-strain relationship for concrete - specimens SCB-1 and SCB-3 (Nie and Cai 2003).

The behavior of concrete in tension is considered as mentioned in the previous section (see Fig. 3.6 on page 21 and Eq. 3.2 on page 20).

The reinforcing steel is modeled as an elasto-plastic material with a strain hardening and yielding plateau beyond the elastic phase as shown in Fig. 3.7. It is symmetrical in tension and compression and the values of yield strength  $f_y$ , Young’s modulus  $E_s$ , strain hardening modulus  $E_{sh}$ , strain at the beginning of the strain hardening  $\epsilon_{sh}$  and the Poisson’s ratio  $\nu$  are  $290 N/mm^2$ ,  $200000 N/mm^2$ ,  $1000 N/mm^2$ , 0.025 and 0.3, respectively.

### 3.3.2 Structural steel

#### 3.3.2.1 Specimen E1, tested by Chapman *et al.* 1964

The material proprieties of the web and flange of the analyzed beam are summarized in Tab. 3.2 and depicted in Fig. 3.9.

Table 3.2: Properties of the structural steel (Chapman *et al.* 1964).

	$E_s [N/mm^2]$	$E_{sh} [N/mm^2]$	$f_y [N/mm^2]$	$f_u [N/mm^2]$	$\epsilon_{sh}/\epsilon_y$	$\nu$
flange	205205	3500	245	458	1	0.3
web	199124	3500	292	453	2.2	0.3

The evolution of the stress-strain curve in the hardening zone follows the constitutive law proposed by Gattesco 1999, as described in Eq. 3.5.

$$\sigma_h = f_y + E_h (\epsilon - \epsilon_{sh}) \left( 1 - E_h \frac{\epsilon - \epsilon_h}{4(f_u - f_y)} \right) \tag{3.5}$$

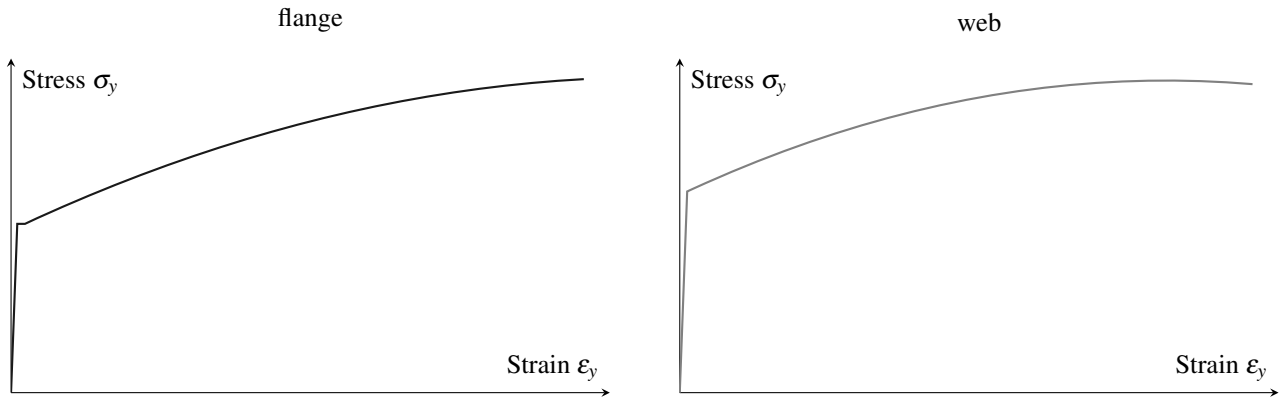


Figure 3.9: Stress-strain relationship for structural steel - specimen E1 (Chapman *et al.* 1964).

where:  $f_y$  and  $f_u$  are the yield and ultimate tensile stresses of the steel component, respectively;  $E_h$  and  $\epsilon_h$  are the strain hardening modulus and the strain at strain hardening of the steel component, respectively.

Due to the noticeable differences that appear among the material properties of the two parts of the steel beam, web and flange, and to the finite element type chosen to model the beam, which is a beam element and it does not allow us to assign more than one material law, the following assumptions are made:

- to obtain a single modulus of elasticity  $E_s$ , for the whole cross-section, the web thickness is modified using Eq. 3.6 as presented in Fig. 3.10.

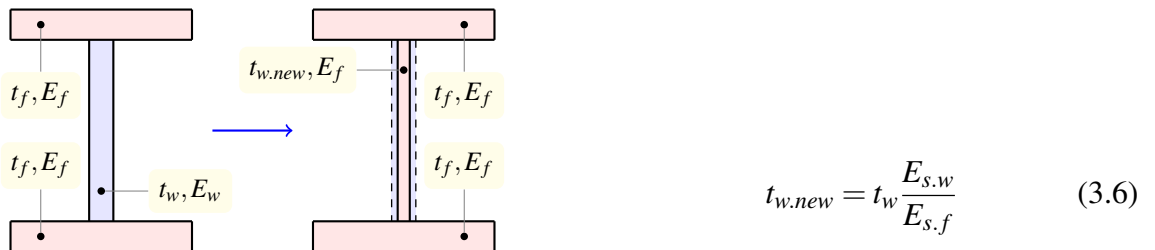


Figure 3.10: Assumption 1: Equivalent section (Chapman *et al.* 1964).

- to obtain a single stress-strain curve for the whole cross-section the following assumption is considered:

$$\sigma_{ech} = \frac{f_{y.f}A_f + f_{y.w}A_w}{A_{tot}} \quad (3.7)$$

where:  $A_f$ ,  $A_w$  and  $A_{tot}$  represent area of the flanges, area of the web and total area of the cross-section, respectively;  $f_{y.f}$  and  $f_{y.w}$  represent the yield strength of the flanges and web.

Similar assumptions are used by other authors, Hradil *et al.* 2012 and Arrayago *et al.* 2015. The equivalent stress-strain curve obtained with Eq. 3.7 is shown in Fig. 3.11.

3.3.2.2 Specimens SCB-1 and SCB-3, tested by Nie and Cai 2003

The structural steel is modeled as an elasto-plastic material with a strain hardening and yielding plateau beyond the elastic phase as shown in Fig. 3.7. It is symmetrical in tension and compression and the values of yield strength  $f_y$ , Young’s modulus  $E_s$ , strain hardening modulus  $E_{sh}$ , strain at the beginning of the strain hardening  $\epsilon_{sh}$  and the Poisson’s ratio  $\nu$  are  $310 \text{ N/mm}^2$ ,  $200000 \text{ N/mm}^2$ ,  $1000 \text{ N/mm}^2$ ,  $0.025$  and  $0.3$ , respectively.

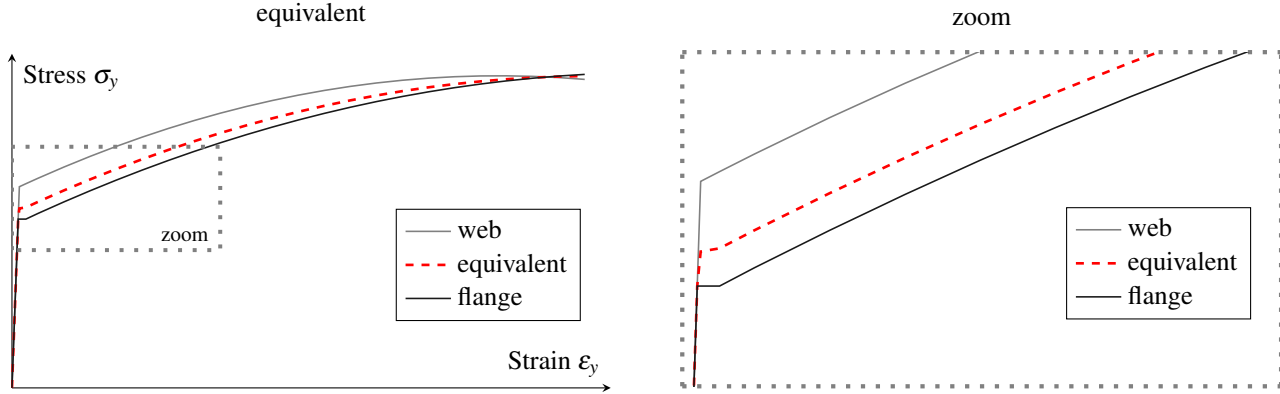


Figure 3.11: Assumption 2: Equivalent stress-strain relationship for structural steel (Chapman *et al.* 1964).

3.3.3 Stud shear connectors

3.3.3.1 Specimen E1, tested by Chapman et al. 1964

The shear connectors constitutive law introduced in the finite element model is experimentally determined from push-out tests done by Chapman *et al.* 1964. A typical constitutive law in terms of force and displacement is depicted in Fig. 3.12.

3.3.3.2 Specimens SCB-1 and SCB-3, tested by Nie and Cai 2003

Due to the absence of the experimental data the shear connectors constitutive law is described using the relation proposed by Ollgaard *et al.* 1971 as described in Eq. 3.8.

$$P = P_u(1 - e^{-ns})^m \tag{3.8}$$

where:  $P$  and  $s$  are the shear force on a stud and the slip at the steel-concrete interface, respectively; the parameters  $m$  and  $n$  define the shape of the curve, and the typical values used in this study are  $m = 0.558$ ,  $n = 1 \text{ mm}^{-1}$ . The ultimate shear capacity of a stud  $P_u$  is described by Eq. 3.9 (Nie, Cai, *et al.* 2007).

$$P_u = \min \begin{cases} 0.43A_{con}\sqrt{E_c f_c} \\ 0.70A_{con}f_u \end{cases} \tag{3.9}$$

where:  $f_u$ ,  $A_{con}$  and  $E_c$  are the ultimate tensile strength of the shear stud, cross-sectional area of the shear stud and the modulus of elasticity of the concrete that is obtained as  $E_c = 10^5 \left( 2.2 \frac{33}{f_{cu}} \right)$ .

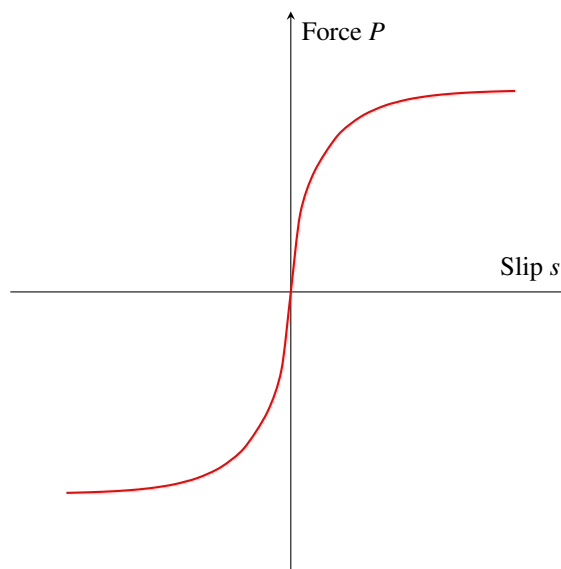


Figure 3.12: A typical shear connectors constitutive law in terms of force and displacement.

## 3.4 Non-linear analysis

A non-linear analysis is carried out using static *Riks* procedure in order to obtain the ultimate load capacity of the beam, that allows us to monitor possible drops in the load-displacement and stress-strain curves. The *Riks* algorithm uses the load magnitude as an additional unknown. Therefore, another quantity must be used to measure the progress of the solution. Abaqus uses the arc-length approach along the static equilibrium path load-displacement space. This approach provides solutions regardless of whether the response is stable or unstable (Abaqus 2011). The material non-linearity is also considered in the analysis.

## 3.5 Validation of the numerical model

### 3.5.1 Specimen E1, tested by Chapman *et al.* 1964

The proposed procedure is validated by comparison against Chapman *et al.* 1964 tests, as well as against alternative numerical studies (Gattesco 1999, Pi *et al.* 2006, El-Lobody *et al.* 2009 and Queiroz *et al.* 2007).

The experiment conducted by Chapman *et al.* 1964 consisted of simply supported composite beams in which the number of shear connectors were placed along the whole length of the specimen including the overhang regions (see Fig. 3.3 on page 18).

The study by Queiroz *et al.* 2007 is the only one of the above mentioned studies which investigated this aspect and concluded that the shear connectors in the overhang regions should be taken into account when calculating the level of shear connection because they have an influence on the system behavior. On the contrary, the connection level decreases. It is also mentioned that in the case of continuation of the shear connection beyond the beam supports not only the overall response (e.g. shape of the load-deflection curve), but also local results (e.g. slip and stud force distributions along

the beam) can be affected. In spite of previously mentioned, the ultimate load is not significantly influenced.

According to Chapman *et al.* 1964, a more rational test procedure would have been to limit the slab length to the distance between supports. Therefore, the present study neglects the effect of the overhang regions and all the presented results refer to the composite beam between supports. Also needs to be mentioned that in the experimental test the shear studs were provided in two rows, whilst in the proposed procedure in a single row, due to the limitations imposed by the usage of the beam finite element type for the structural steel.

The comparison between the proposed procedure, with and without the slab reinforcement, and the experimental results is presented in Fig. 3.13. Whether the slab reinforcement is considered or not in the numerical model may not influence the result of stiffness, but slightly influence the result of ultimate loading capacity. It can be noticed that the present procedure including the slab reinforcement demonstrate good capabilities of predicting the real behavior of the composite beam.

As it can be seen in Fig. 3.14 the behavior of steel-concrete composite beam predicted by the present analysis is in close agreement with that of finite element analysis presented in other studies.

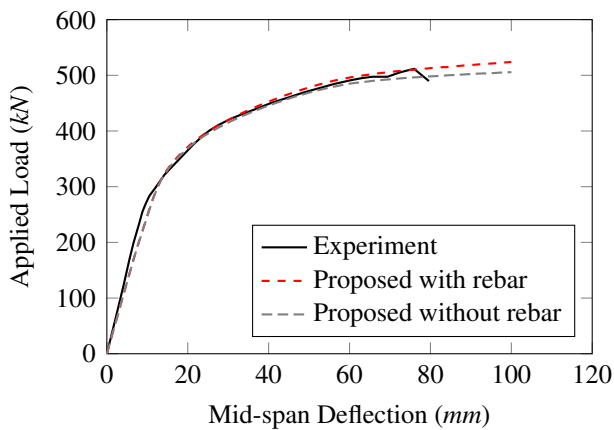


Figure 3.13: Specimen E1: Load vs. mid-span deflection (Chapman *et al.* 1964).

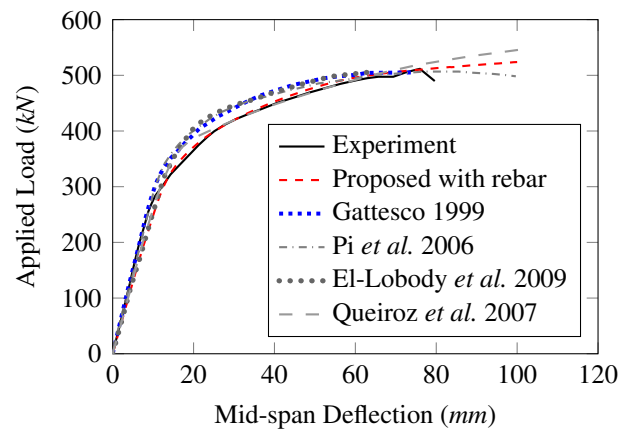


Figure 3.14: Specimen E1: Load vs. mid-span deflection - different procedures.

The effectiveness of the proposed procedure is further assessed by varying the level of shear connection of the model with reinforcing. The results obtained are compared against the predicted curves achieved using a more complex finite element analysis (Queiroz *et al.* 2007). Hereinafter the model with reinforcing will be referred to as “proposed”.

The level of shear connection is determined based on strength of the composite section components (i.e. concrete slab, structural steel and shear connectors). This value is defined as the ratio between the shear connection capacity and the weakest element capacity (concrete slab or steel beam). The level of shear connection for all the analyzed composite beams in this study (i.e. specimens E1, SCB-1 and SCB-3) is based on the material properties taken as the actual material properties of the components (measured values), related to each experimental program (Chapman *et al.* 1964 and Nie and Cai 2003), as suggested by Queiroz *et al.* 2007. Tab. 3.3 summarizes the level of shear connection for specimen E1.

For a better understanding the results against other alternative study (Queiroz *et al.* 2007) were plotted independently for each level of shear connection, as shown in Figs. 3.15 to 3.21.



Table 3.3: Level of shear connection of specimen E1.

Level of shear connection	148% <sup>a</sup>	136%	130%	118%	100% <sup>b</sup>	81%	79%	47%
Number of studs	100	92	88	80	68	60	48	32

<sup>a</sup> The tested beam with overhanging regions, which are neglected in the present study.

<sup>b</sup> Represents the case of full shear connection. Below this value, the partial shear connection case appears.

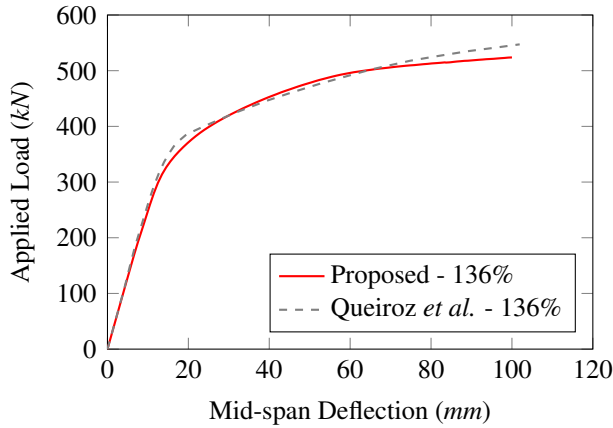


Figure 3.15: Specimen E1: Load vs. mid-span deflection - level of shear connection: 136%.

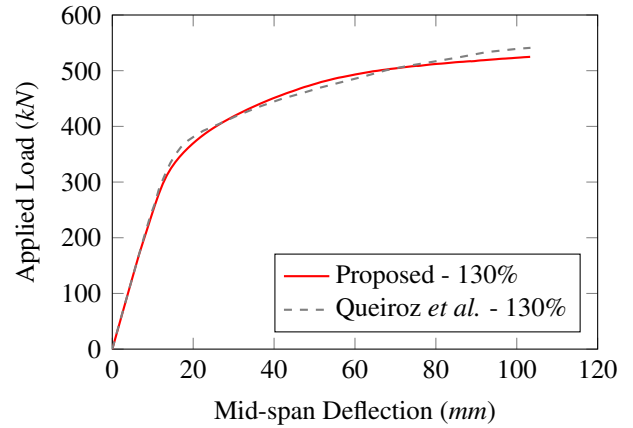


Figure 3.16: Specimen E1: Load vs. mid-span deflection - level of shear connection: 130%.

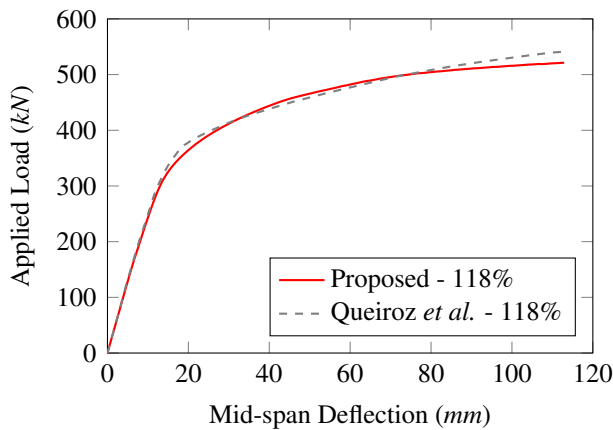


Figure 3.17: Specimen E1: Load vs. mid-span deflection - level of shear connection: 118%.

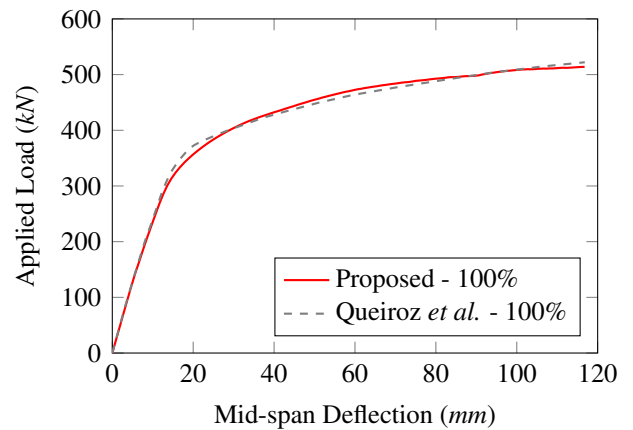


Figure 3.18: Specimen E1: Load vs. mid-span deflection - level of shear connection: 100%.

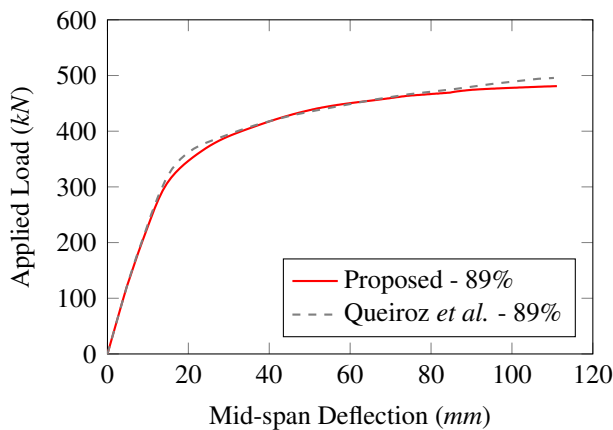


Figure 3.19: Specimen E1: Load vs. mid-span deflection - level of shear connection: 89%.

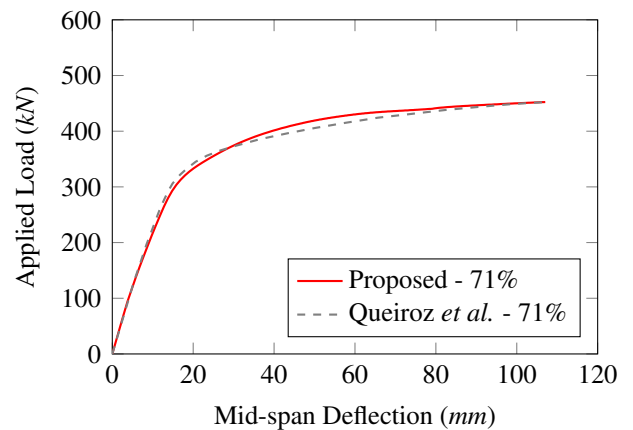


Figure 3.20: Specimen E1: Load vs. mid-span deflection - level of shear connection: 71%.

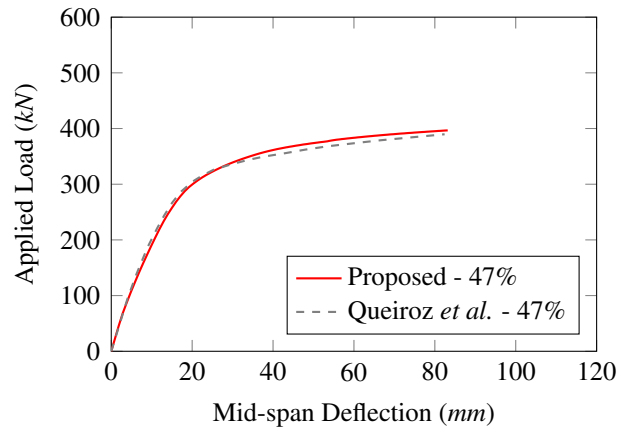


Figure 3.21: Specimen E1: Load vs. mid-span deflection  
- level of shear connection: 47%.

As it can be seen, the results agree fairly well and the proposed method accurately predicts the nonlinear behavior obtained with a more complex analysis done by Queiroz *et al.* 2007, in which the structural steel and the concrete slab are modeled with shell and solid finite element types.

The load-deflection curves for all degrees of shear connection are depicted in Fig. 3.22. It can be observed that, decreasing the level of shear connection makes the system become more flexible, with reduced strength and stiffness.

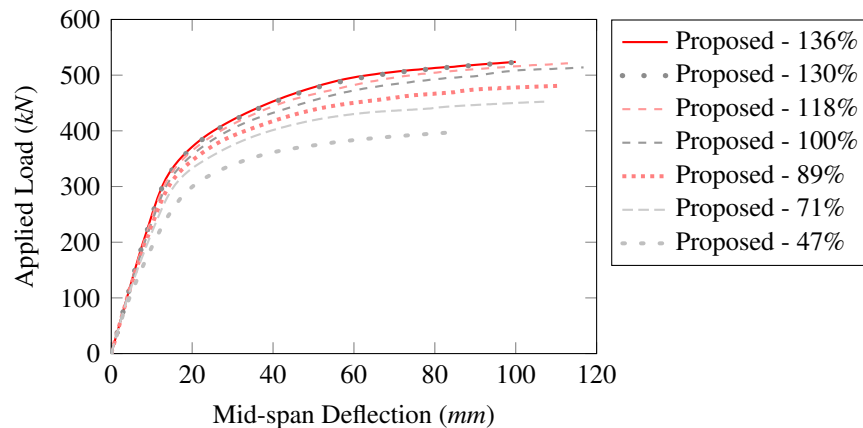


Figure 3.22: Specimen E1: Load vs. mid-span deflection  
- all levels of shear connection.

### 3.5.2 Specimens SCB-1 and SCB-3, tested by Nie and Cai 2003

The proposed procedure is validated by comparison against Nie and Cai 2003 tests, as well as against alternative numerical studies Nie, Tao, *et al.* 2011. Tab. 3.4 presents the level of shear connection for specimen SCB-1 and SCB-3, respectively considering the material properties related to the experimental program, as aforementioned.

Due to the different types of loading, two-point loading for SCB-1 (see Fig. 3.1 on page 18) and one-point loading for SCB-3 (see Fig. 3.2 on page 18), the distance between connectors in the experimental program was different. The pitch for SCB-1 was 115 mm in shear span and 125 mm in bending region, and for SCB-3 148 mm along the whole length.

As it can be seen in Fig. 3.23 the present method accurately predicts the nonlinear behavior and ultimate load capacity and the results obtained are in good agreement with results derived from other finite element procedures, as shown in Fig. 3.24.

Table 3.4: Level of shear connection of specimens SCB-1 and SCB-3.

Level of shear connection	139%	119%	100% <sup>a</sup>	88%	70%	46%
SCB-1						
Number of studs	46	39	33	29	23	15
SCB-3						
Number of studs	36	31	26	23	18	12

<sup>a</sup> The experimentally tested beam and represents the case of full shear connection. Below this value, the partial shear connection case appears.

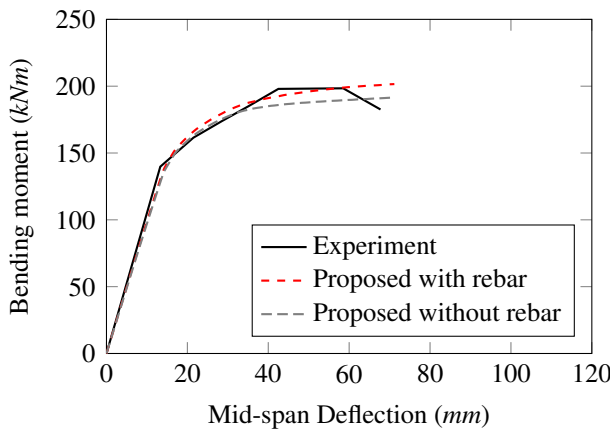


Figure 3.23: Specimen SCB-1: Bending moment vs. mid-span deflection (Nie and Cai 2003).

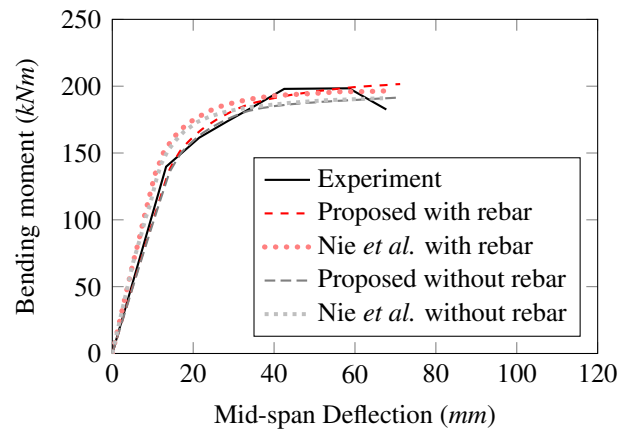


Figure 3.24: Specimen SCB-1: Bending moment vs. mid-span deflection - different procedures.

The proposed procedure for specimen SCB-3 is quite accurate, even with the differences that appear on the elastic branch, as show in Fig. 3.25. These differences may occur due to simplifications made in the finite element analysis and also to absence of some experimental data. Nevertheless, the proposed procedure can closely predict the ultimate load capacity and compared to other procedures (Nie, Tao, *et al.* 2011) it can be assumed that is more accurate, as presented in Fig. 3.26.

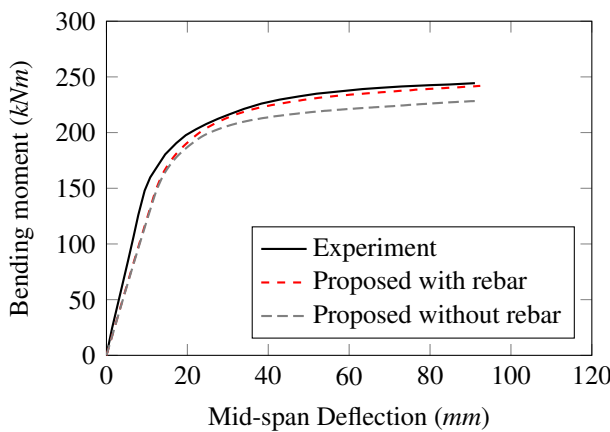


Figure 3.25: Specimen SCB-3: Bending moment vs. mid-span deflection (Nie and Cai 2003).

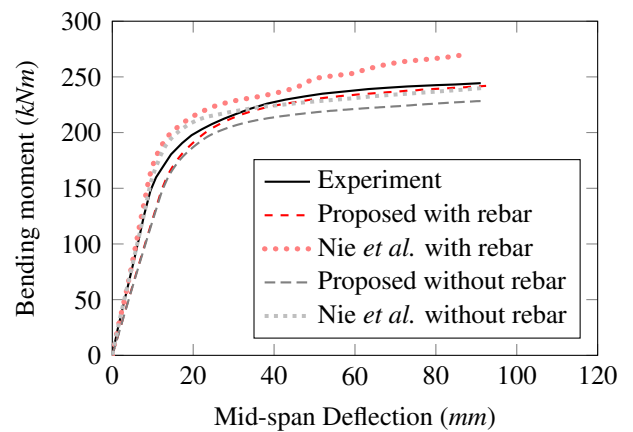


Figure 3.26: Specimen SCB-3: Bending moment vs. mid-span deflection - different procedures.

The bending moment-deflection curves for all degrees of shear connection for both specimens tested by Nie and Cai 2003 are depicted in Fig. 3.27 and Fig. 3.28, respectively. It can be easily observed that, increasing the number of shear connectors does not lead to significant increases in ultimate load capacity.

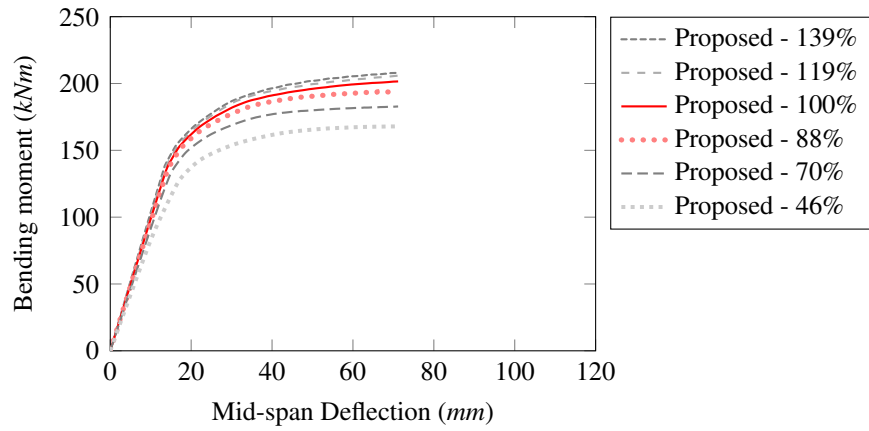


Figure 3.27: Specimen SCB-1: Bending moment vs. mid-span deflection - all levels of shear connection.

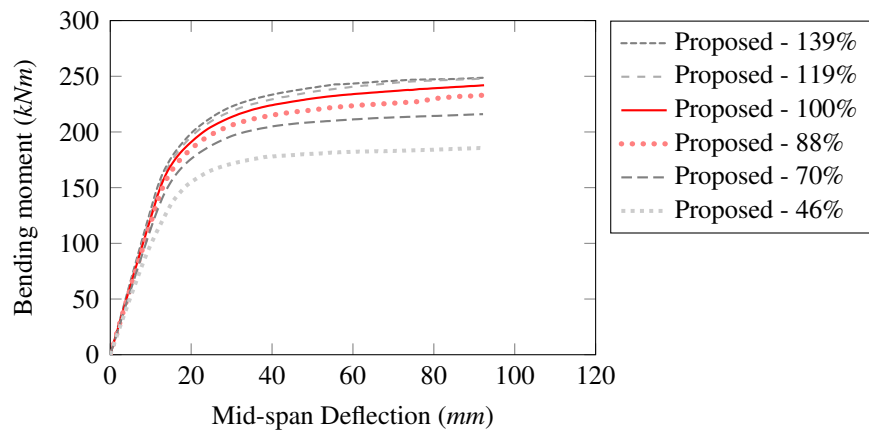


Figure 3.28: Specimen SCB-3: Bending moment vs. mid-span deflection - all levels of shear connection.

# Chapter 4

## Parametric studies

### 4.1 Attainment of full shear connection according to different design codes

A brief description of the procedure for determining the number of shear connectors in order to achieve full shear connection is carried out in this current section.

Three design codes for steel-concrete composite structures from different regions of the world, Europe, Australia and United States of America, are presented and compared. Each code is presented with respect to its notations.

#### 4.1.1 Europe - EN 1994-1-1 2004

The Eurocode (EC) is a set of technical rules developed by the European Committee for Standardization for the structural design of construction works in the European Union and is divided in ten parts.

According to the fourth part of the Eurocode, also known as Eurocode 4: *Design of composite steel and concrete structures*, the required number of shear connectors in case of full shear connection is expressed by Eq. 4.1, which represents the ratio between the minimum element capacity (i.e. concrete slab or steel beam) (Eq. 4.2) and the design shear capacity of a shear connector (Eq. 4.3).

$$n_f = \frac{N}{P_{Rd}} \quad (4.1)$$

where:

- $n_f$  - number of connectors for full shear connection.
- $N$  - design shear force for the ultimate limit state.
- $P_{Rd}$  - design value of the shear resistance of a single connector.

$$N = \min \begin{cases} N_a \\ N_c \end{cases} \quad (4.2)$$

where:

- $N_a$  - design value of the normal force in the structural steel section of a composite beam.
- $N_c$  - design value of the compressive normal force in the concrete slab of a composite beam.

$$N_c = h_c b_{eff} 0.85 \frac{f_{ck}}{\gamma_c}$$

where:

- $h_c$  - depth of the concrete encasement to a steel section.
- $b_{eff}$  - total effective width.
- $f_{ck}$  - characteristic value of the cylinder compressive strength of concrete at 28 days.
- $\gamma_c$  - partial factor for concrete.

$$N_a = A_a f_{yd}$$

where:

- $A_a$  - cross-sectional area of the structural steel section.
- $f_{yd}$  - design value of the yield strength of structural steel.

$$P_{Rd} = \min \left\{ \begin{array}{l} \frac{0.8 f_u \phi d^2}{\gamma_w} \\ \frac{0.29 \alpha d^2 \sqrt{f_{ck} E_{cm}}}{\gamma_w} \end{array} \right. \quad (4.3)$$

where:

- $\alpha$  - coefficient.

$$\alpha = \begin{cases} 0.2 \left( \frac{h_{sc}}{d} + 1 \right) & , \text{for: } 3 \leq \frac{h_{sc}}{d} \leq 4 \\ 1 & , \text{for: } 4 < \frac{h_{sc}}{d} \end{cases}$$

- $h_{sc}$  - height of the stud.
- $\gamma_w$  - partial factor.
- $d$  - diameter of the shank of the stud,  $16 \text{ mm} \leq d \leq 25 \text{ mm}$ .
- $f_{ck}$  - characteristic cylinder compressive strength of the concrete at the age considered, of density not less than  $1750 \text{ kg/m}^3$ .
- $f_u$  - specified ultimate tensile strength of the material of the stud but not greater than  $500 \text{ N/mm}^2$ .

#### 4.1.2 Australia - AS-2327.1 2003

The Australian Standard (AS) represents a set of technical standards developed by Standards Australia.

According to AS-2327.1 2003, also known as *Australian Standard - Composite structures Part 1: Simply supported beams*, the required number of shear connectors in case of full shear connection is expressed by Eq. 4.4, which represents the ratio between the minimum element capacity (Eq. 4.5) and the shear strength of the studs (Eq. 4.6).

$$n_i = \frac{F_{cp}}{f_{ds}} \quad (4.4)$$

where:

- $n_i$  - minimum number of shear connectors (with the same design shear capacity  $f_{ds}$ ) between a potentially critical cross-section  $i$  and the ends of the beam to satisfy the design requirement  $\phi M_{bv} \geq M^*$ .
- $F_{cp}$  - compressive force in concrete slab at a cross-section with partial shear connection where  $\gamma \leq 0.5$  at the strength limit state.
- $f_{ds}$  - design shear capacity of a shear connector.

$$F_{cp} = \beta F_{cc} \quad (4.5)$$

where:

- $\beta$  - degree of shear connection at a cross-section.
- $F_{cc}$  - compressive force in concrete slab at a cross-section with complete shear connection where  $\gamma \leq 0.5$  at the strength limit state.

$$F_{cc} = F_{st} \quad , \text{ in the current case because } F_{st} \leq F_{c1}$$

$$F_{st} = (A_{f1} + A_{f2})f_{yf} + A_w f_{yw}$$

where:

- $F_{st}$  - tensile force in steel beam.
- $A_{fi}$  - cross-sectional area of a flange of the steel beam.
- $A_w$  - cross-sectional area of the web(s) of the steel beam.
- $f_{yf}$  - yield strength of the flange of the steel beam.
- $f_{yw}$  - yield strength of the web of the steel beam.

$$F_{c1} = 0.85f'_c b_{cf}(D_c - h_r)$$

where:

- $F_{c1}$  - Longitudinal compressive capacity of concrete slab.
- $f'_c$  - 28 day characteristic compressive cylinder strength of concrete.
- $b_{cf}$  - effective width of the concrete slab compression flange.
- $D_c$  - overall depth of a concrete slab including the thickness of any profiled steel sheeting if present.
- $h_r$  - height of steel ribs in profiled steel sheeting.

$$f_{ds} = \phi k_n f_{vs} \quad (4.6)$$

where:

- $f_{ds}$  - design shear capacity of a shear connector.
- $\phi$  - capacity factor for the strength limit state.
- $k_n$  - load-sharing factor.
- $f_{vs}$  - nominal shear capacity of a shear connector.

$$f_{vs} = \min \left\{ \begin{array}{l} 0.63d_{bs}^2 f_{uc} \\ 0.31d_{bs}^2 \sqrt{f'_{cj} E_c} \end{array} \right.$$

where:

- $f_{uc}$  - tensile strength of the shear-connector material used in design.
- $f'_c$  - 28 day characteristic compressive cylinder strength of concrete.
- $E_c$  - elastic modulus of the slab concrete.
- $d_{bs}$  - nominal shank diameter of a headed-stud or a high-strength structural bolt shear connector.

### 4.1.3 United States of America - AISC-LRFD 1994

The American Institute of Steel Construction (AISC) is an Institute that publishes manuals, textbooks, specifications and technical booklets. One of the best known and most widely used manual, also in this current study, is the *Load and Resistance Factor Design Manual (LRFD)*, which holds a highly respected position in engineering literature. According to its *Part 2 - Essentials of LRFD, Chapter I - Composite Members*, the number of shear connectors in order to achieve full shear connection is described by Eq. 4.7, which represents the ratio between the minimum horizontal shear force to be transferred (Eq. 4.8) and the shear strength of one connector (Eq. 4.9).

$$n = \frac{V_h}{Q_n} \quad (4.7)$$

where:

- $n$  - number of shear connectors required between a point of maximum moment and the nearest location of zero moment.
- $V_h$  - total horizontal shear force to be transferred.
- $Q_n$  - shear strength of one connector.

$$V_h = \min \begin{cases} F_c \\ F_s \end{cases} \quad (4.8)$$

where:

- $F_c$  - strength of the concrete slab.
- $F_s$  - strength of the structural steel.

$$F_c = 0.85f'_cA_c$$

where:

- $f'_c$  - specified compressive strength of the concrete.
- $A_c$  - cross-sectional area of concrete.

$$F_s = A_sF_y$$

where:

- $A_s$  - cross-sectional area of structural steel.
- $F_y$  - specified minimum yield stress of the structural steel shape.

$$Q_n = \min \begin{cases} 0.5A_{sc}\sqrt{f'_cE_c} \\ A_{sc}F_u \end{cases} \quad (4.9)$$

where:

- $A_{sc}$  - cross-sectional area of a stud shear connector.
- $f'_c$  - specified compressive strength of concrete.
- $E_c$  - modulus of elasticity of concrete.
- $F_u$  - minimum specified tensile strength of a stud shear connector.



#### 4.1.4 Differences between the design codes

A calculation based on the aforementioned design codes, in order to achieve full shear connection for the analyzed specimens in Chapter 3, is presented in Tab. 4.1.

Table 4.1: Differences between design codes.

Specimen	Standard	$F_{steel}$	$F_{concrete}$	$P_{con.1}$	$P_{con.2}$	$n_{sec}$	$n_{tot}$	$n_{exp}$	$n_{exp}/n_{tot}$
E1	EC	2177	3441	45	39	57	114		0.60
	AS	2177	5162	57	50	49	98	68	0.69
	LRFD	2177	5162	70	63	35	70		0.97
SCB-1	EC	1091	785	78	68	12	31		1.06
	AS	1091	1177	98	84	15	38	33	0.87
	LRFD	1091	1177	122	117	10	26		1.27
SCB-3	EC	1091	1259	78	68	17	34		0.76
	AS	1091	1884	98	84	15	30	26	0.87
	LRFD	1091	1884	122	117	10	20		1.30

where  $F_{steel}$  is the tensile force in steel beam,  $F_{concrete}$  is the compressive force in concrete slab,  $P_{con.1}$  is the shear resistance of a single connector considering connector failure,  $P_{con.2}$  is the shear resistance of a single connector considering connector failure,  $n_{sec}$  is the minimum number of shear studs for a potentially critical cross-section,  $n_{tot}$  is the total number of shear studs along the whole beam and  $n_{exp}$  is the number of shear studs used in the experimental program.

The values of  $F_{steel}$ ,  $F_{concrete}$ ,  $P_{con.1}$ ,  $P_{con.2}$  are in (kN).

According to Tab. 4.1 the strength value of the concrete,  $F_{concrete}$ , is equally appreciated by both Australian and American code, while restrictive tendency is observed in European code. The difference appears due to the partial safety factor for concrete  $\gamma_c$ , which is not present in the other two codes. Its value depend on the design situation: 1.5 for persistent and transient and 1.2 for accidental. On the other hand, the strength value of the structural steel,  $F_{steel}$ , is identically appreciated by all the presented design codes.

In terms of failure modes, all the three codes are expecting that the concrete will crack before the ultimate strength is achieved in the shear studs (the value of  $P_{con.2}$  is in all the cases less than  $P_{con.1}$ ). It appears that both the European and the Australian norms are conservative in terms of the shear capacity of a single connector, hence increasing the total number is required. Also, it can be noticed that the values obtained using the Australian design prescriptions, for the shear resistance of a single connector for both failure cases, concrete and connector, are close to the mid values of European and American codes.

In conclusion the tendency of restrictiveness becomes higher from the European to Australian norm and from the Australian to the American norm.

## 4.2 Influence of the slab concrete strength on the composite beam response

The main focus of this section is based on load-deflection curves for different slab concrete strengths, with the same value being used in the associated push-out specimen (Chapman *et al.* 1964). More details about the model can be found in Chapter 3.

Fig. 4.1 shows the finite element model results and Tab. 4.2 the influence of the slab concrete strength on the steel-concrete composite beam response. The slab concrete strength varies from  $0.70f_c$  to  $1.30f_c$ .

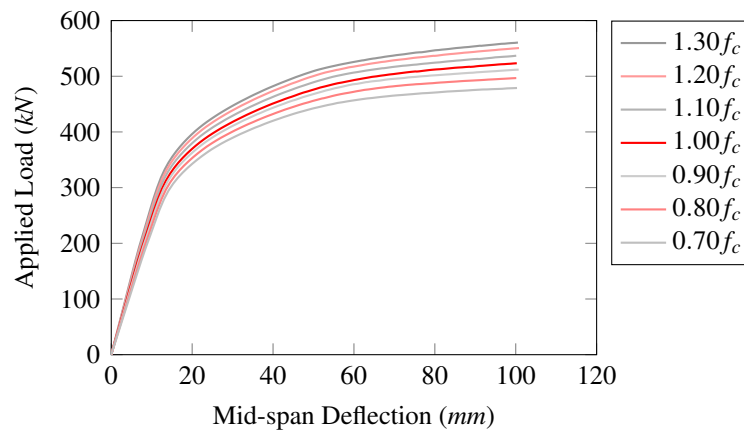


Figure 4.1: Load vs. mid-span deflection - for different concrete slab strengths.

Table 4.2: Influence of the slab concrete strength on the composite beam.

concrete slab strength							
$f_c$ (%) <sup>a</sup>	$0.70f_c$	$0.80f_c$	$0.90f_c$	$1.00f_c$	$1.10f_c$	$1.20f_c$	$1.30f_c$
$f_c$ ( $N/mm^2$ )	22.88	26.14	29.41	32.68	35.95	39.22	42.48
ultimate load							
$P_u$ (%) <sup>b</sup>	$0.92P_u$	$0.95P_u$	$0.98P_u$	$1.00P_u$	$1.02P_u$	$1.05P_u$	$1.07P_u$
$P_u$ (kN)	470.48	487.54	501.68	512.22	523.83	536.59	545.83

where  $f_c$  and  $P_u$  represent the cylinder strength of the concrete and the ultimate load, respectively.

<sup>a</sup> The value of  $1.0f_c$  is considered as a reference, because represents the value used in the experimental program.

<sup>b</sup> The value of  $1.0P_u$  is considered as a reference and its value correspond to the maximum displacement obtained in the experimental program.

Analyzing the obtained curves it can be concluded that an increase in the concrete slab strength resulted in a stiffer system and in an increase in the moment capacity of the steel-concrete composite beam. Nevertheless, the former effect seems to be less significant than the latter one.

## 4.3 Influence of the slab concrete width on the composite beam response

An important aspect for a correct design of steel-concrete composite beams is the effective width of the concrete slab. Intense research on this topic was developed by Sedlacek *et al.* 1993, Dezi *et al.* 2001, Amadio and Fragiaco 2002 and Amadio, Fedrigo, *et al.* 2004. Due to the shear strains the cross-section does not remain plane after deformation. This phenomenon is known as the *shear-lag* effect and is influenced by the behavior of the materials and geometric parameters, such as the span length.

Further, the specimen E1 (Chapman *et al.* 1964) is subjected to variations of the effective width of the slab concrete, from  $0.40b_c$  to  $1.60b_c$ .

Fig. 4.2 shows the finite element model results and Tab. 4.3 the influence of the slab concrete width on the composite beam response.

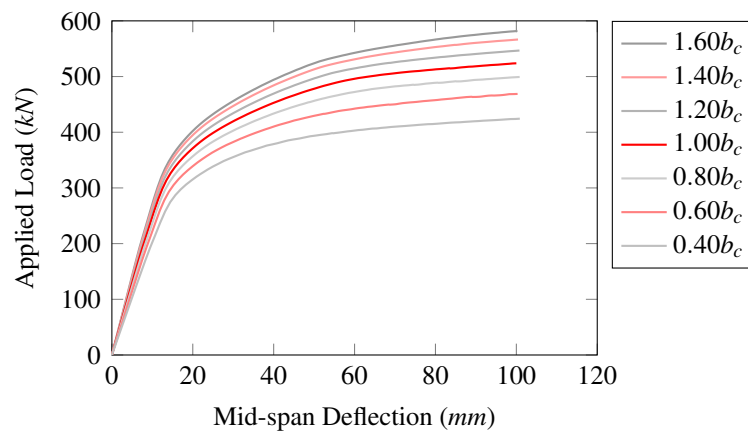


Figure 4.2: Load vs. mid-span deflection - for different concrete slab effective widths.

Table 4.3: Influence of the slab concrete width on the composite beam.

concrete slab width							
$b_c$ (%) <sup>a</sup>	$0.40b_c$	$0.60b_c$	$0.80b_c$	$1.00b_c$	$1.20b_c$	$1.40b_c$	$1.60b_c$
$b_c$ (mm)	487.68	731.52	975.36	1219.20	1463.04	1706.88	1950.72
ultimate load							
$P_u$ (%) <sup>b</sup>	$0.81P_u$	$0.89P_u$	$0.95P_u$	$1.00P_u$	$1.04P_u$	$1.08P_u$	$1.10P_u$
$P_u$ (kN)	414.70	457.47	488.59	512.22	533.345	552.885	565.49

where  $b_c$  and  $P_u$  represent the width of the concrete slab of the composite beam and the ultimate load, respectively.

<sup>a</sup> The value of  $1.00b_c$  is considered as a reference, because represents the value used in experimental program.

<sup>b</sup> The value of  $1.0P_u$  is considered as a reference and its value correspond to the maximum displacement obtained in the experimental program.

It can be noticed that the influence of the effective width of concrete slab on the behavior of steel-concrete composite beam is significant and an adequate approach is required to assess its structural effects.

### 4.4 Mesh-sensitivity analysis

In order to investigate the influence of the mesh on the simulation results, a set of analyzes with different size of mesh elements are carried out on specimen E1 (Chapman *et al.* 1964). The variation of the mesh is presented in Figs. 4.3 to 4.6.

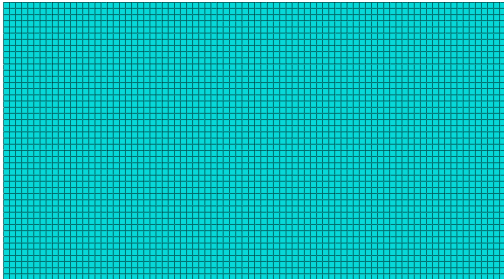


Figure 4.3: Mesh size 15.

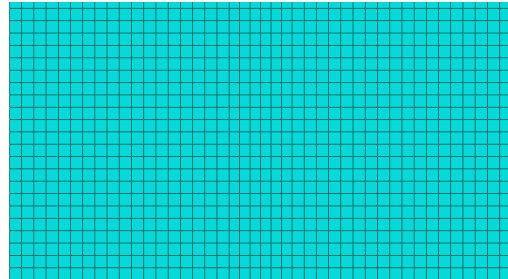


Figure 4.4: Mesh size 30.

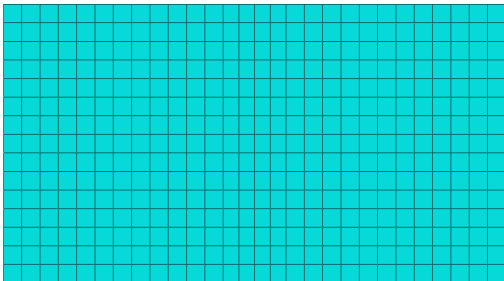


Figure 4.5: Mesh size 45.

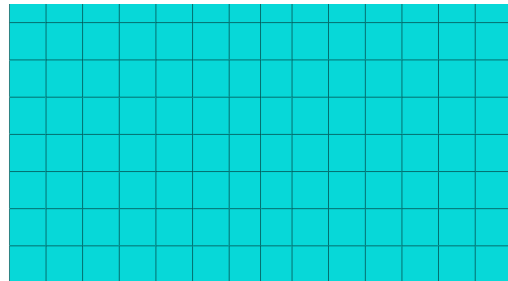


Figure 4.6: Mesh size 90.

It can be clearly seen that the numerical models may be insensitive to the mesh size, since all the predicted curves in Fig. 4.7 have given almost the same results. The mesh size only slightly influences the smoothness of the post-cracking curve, but this is not quite important for the simulation of the global behavior of composite beams (Nie, Tao, *et al.* 2011).

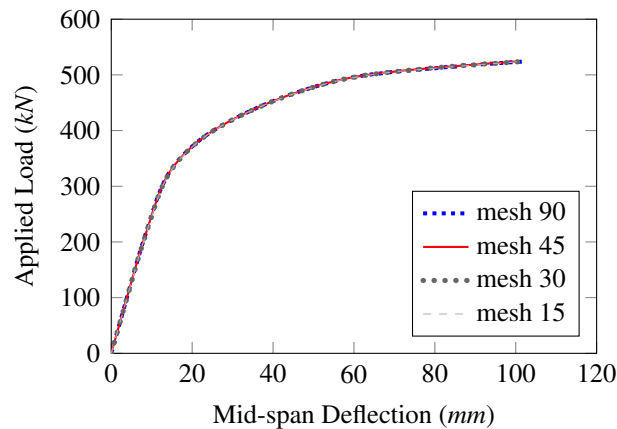


Figure 4.7: Mesh-sensitivity analysis of specimen E1 (Chapman *et al.* 1964).

## 4.5 Fracture energy effects

The purpose of this section is to present the effect of different methods of defining the tension stiffening part of concrete. In this respect, a set of finite element analyzes are carried out on specimen E1 experimentally tested by Chapman *et al.* 1964.

The proposed procedure, as show in Fig. 4.8 and presented in Chapter 3, was subjected to this effect, but the results were not as expected, due to the fact that the concrete slab is modeled with shell finite elements. Therefore, two new models were developed, using different types of finite element, as shown in Fig. 4.9 and Fig. 4.10. The finite element types are presented in Tab. 4.4.

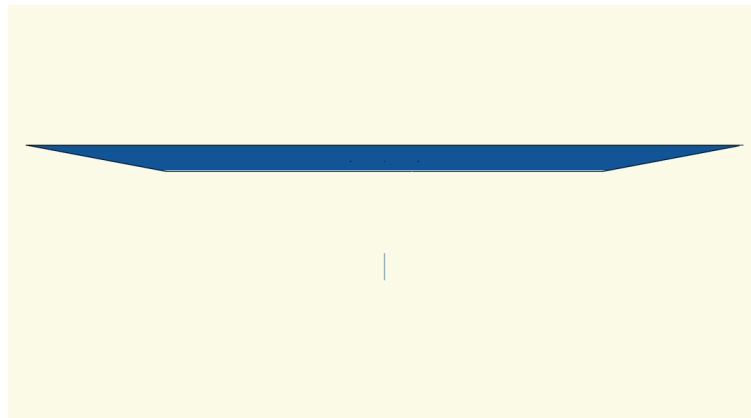


Figure 4.8: Proposed procedure E1.

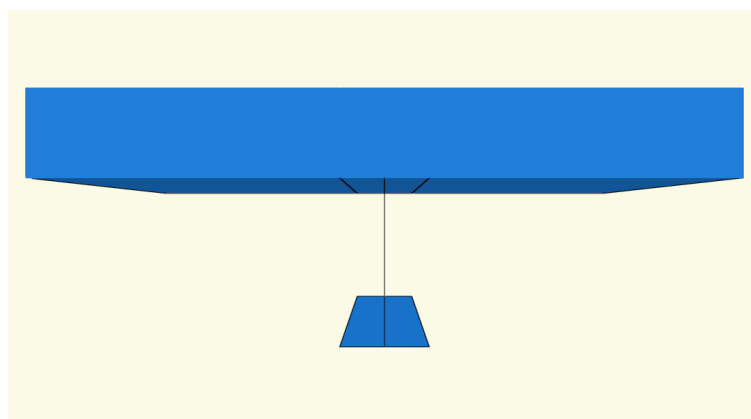


Figure 4.9: Proposed procedure E1-sc.

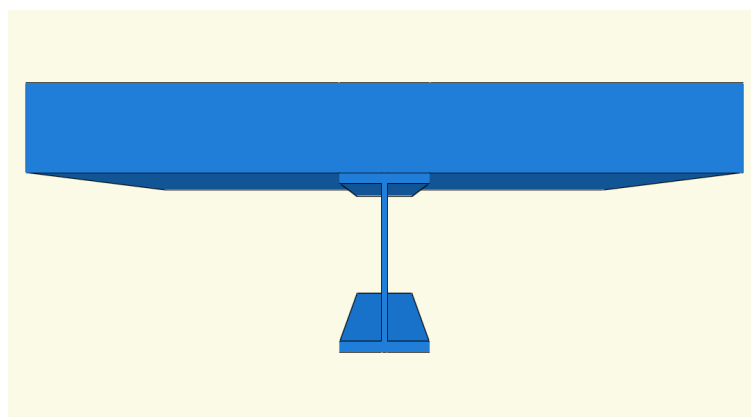


Figure 4.10: Proposed procedure E1-cc.

Table 4.4: Differences between the proposed procedures.

Specimen	Structural steel		Concrete slab	
	FE name	FE type	FE name	FE type
E1 <sup>a</sup>	beam	B31	shell	S4R
E1-sc	shell	S4R	solid	C3D8R
E1-cc	solid	C3D8R	solid	C3D8R

<sup>a</sup> Proposed procedure, see Chapter 3.

The finite element types used to model the different structural components of the two new developed models, presented in this section, are: eight-node brick elements with reduced integration, C3D8R, for concrete slab and/or steel beam and two-node three-dimensional linear truss elements, T3D2, for reinforcing steel. The reinforcement is embedded in the solid element which represents the slab, as shown in Fig. 4.11. Also, it is needed to be mentioned that in both proposed procedures, E1-sc and E1-cc, the shear studs were disposed on two rows, as were in the experimental program (Chapman *et al.* 1964). No other difference, besides the aforesaid, exists between the proposed procedures.

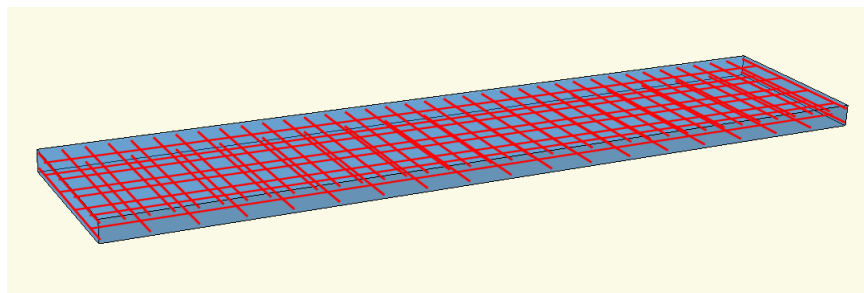


Figure 4.11: Reinforcement embedded in concrete slab.

The Abaqus software package (Abaqus 2011) offers two methods of introducing the tension stiffening part of concrete, one by post-failure stress-strain relationships and another by defining the fracture energy cracking criterion.

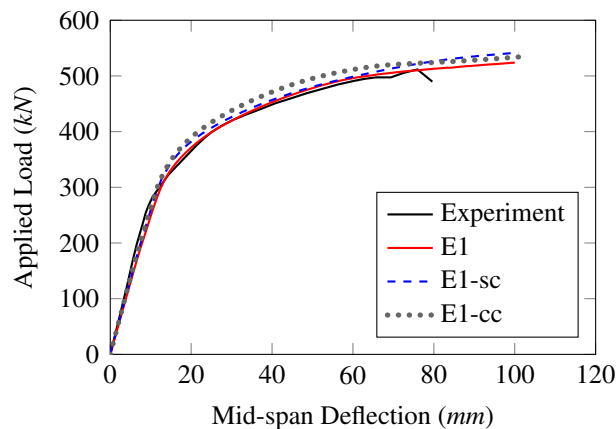


Figure 4.12: Load vs. mid-span deflection - different proposed procedures.

The post-failure stress-strain relationship assumed in the numerical model is the one presented

in Fig. 4.12 on page 21). The obtained results using this method for tension stiffening are presented in Fig. 4.12. Differences start to appear when solid finite elements are used because these types of finite element exhibit a stiffer behavior usually. Besides that, it can be assumed that the presented procedures are in good agreement with the experiment.

When there is no reinforcement in significant regions of the model, the tension stiffening approach described in Chapter 3 will introduce unreasonable mesh sensitivity into the results.

In order to avoid these, the fracture energy cracking criterion was applied. The energy required to open a unit area of crack,  $G_f$ , is defined by Hillerborg *et al.* 1976 as a material parameter, using fracture mechanics concepts. With this approach the concrete's brittle behavior is characterized by a stress-displacement response rather than a stress-strain response. Under tension a concrete specimen will crack across some section. After it has been pulled apart sufficiently for most of the stress to be removed (so that the undamaged elastic strain is small), its length will be determined primarily by the opening at the crack. The opening does not depend on the specimen's length (Abaqus 2011).

The fracture energy cracking criterion can be defined by means of displacement or energy (Fig. 4.13) in Abaqus. The former method requires pairs of post-failure stress-displacement, whereas the latter is defined by means of yield stress and fracture energy.

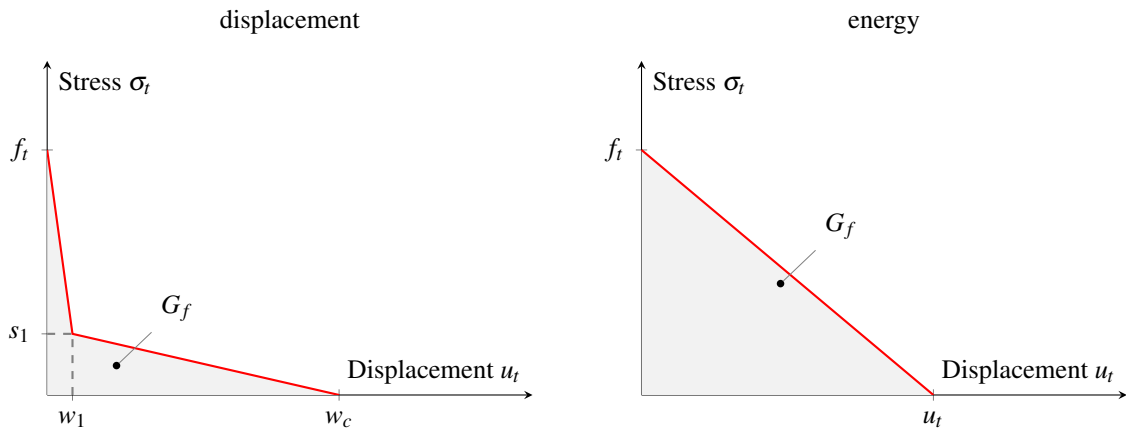


Figure 4.13: The fracture energy cracking criterion: (left) displacement; (right) energy.

In the case of using displacement as fracture energy cracking criterion, a bi-linear diagram recommended by (Brühwiler *et al.* 1990) is used in the present study. The optimal stress and crack opening values at the break point for concrete with 25 mm maximum aggregates are:

$$\begin{aligned} s_1 &= 0.4f_t \\ w_1 &= 0.80 \frac{G_f}{f_t} \end{aligned} \quad (4.10)$$

and for structural concrete:

$$\begin{aligned} s_1 &= \frac{f_t}{4} \\ w_1 &= 0.75 \frac{G_f}{f_t} \end{aligned} \quad (4.11)$$

In the other case, the cracking displacement at which complete loss of strength takes place is,

therefore,  $u_{t0} = \frac{2G_f}{f_{t0}}$  (Abaqus 2011). This model assumes a linear loss of strength after cracking.

All the parameters of concrete's constitutive law are obtained using a set of relations based on the nominal strength of concrete obtained from cylinder compressive tests, suggested by Kadlec *et al.* 2015. The parameters are described by Eq. 4.12.

$$\begin{aligned}
 f_c &= -0.85f_{cu} \quad , \text{cylinder compressive strength} \\
 f_t &= -0.24f_{cu}^{\frac{2}{3}} \quad , \text{tensile strength} \\
 E_c &= (6000 - 15.5f_{cu}) \sqrt{f_{cu}} \quad , \text{initial elastic modulus} \\
 G_f &= G_{f0} \frac{f_c}{10}^{0.7} \quad , \text{fracture energy}
 \end{aligned}
 \tag{4.12}$$

where:  $f_{cu}$  represents the characteristic compressive cubic strength and is taken as the measured value, related to the experimental program (Chapman *et al.* 1964);  $G_{f0}$  depends on  $d_{max}$  which is the maximum diameter of aggregate:

$$G_{f0} = \begin{cases} 25 \frac{N}{mm^2} & , \text{if } d_{max} = 8 \text{ mm} \\ 30 \frac{N}{mm^2} & , \text{if } d_{max} = 16 \text{ mm} \\ 58 \frac{N}{mm^2} & , \text{if } d_{max} = 32 \text{ mm} \end{cases}$$

In the present study Eq. 4.11 is used and the diameter of the aggregate is considered 32 mm.

The obtained results, using the displacement and the energy, as a fracture energy cracking criterion, are shown in Fig. 4.14 and Fig. 4.15, respectively.

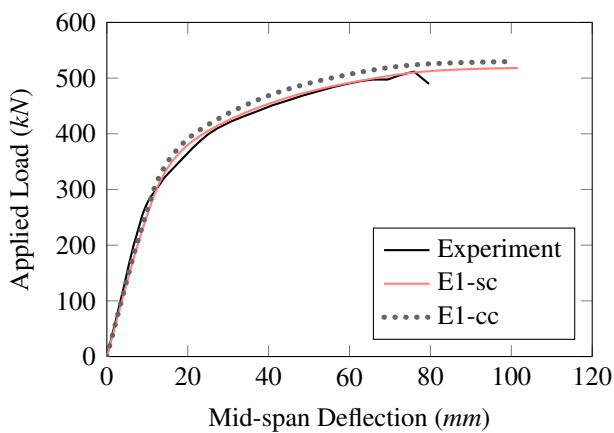


Figure 4.14: Load vs. mid-span deflection - fracture energy cracking criterion: displacement.

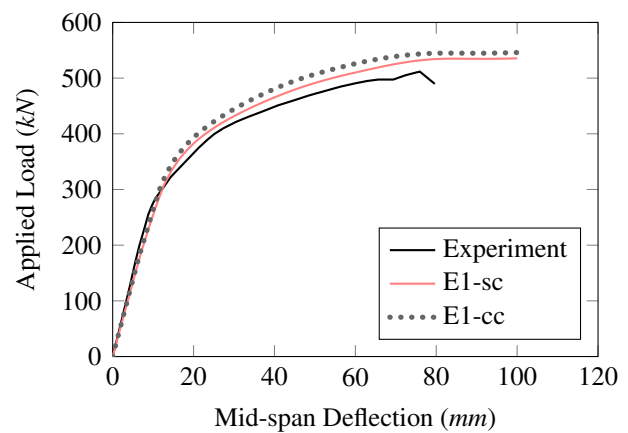


Figure 4.15: Load vs. mid-span deflection - fracture energy cracking criterion: energy.

The results obtained introducing the tension stiffening by means of a post-failure stress-strain relationship and by applying both fracture energy cracking criteria, available in Abaqus software



package, displacement and energy, for each proposed procedure, presented in the current section, are depicted individually to observe better the behavior of the models. The results for the proposed procedure, E1-sc, are depicted in Fig. 4.16 and for E1-cc in Fig. 4.17.

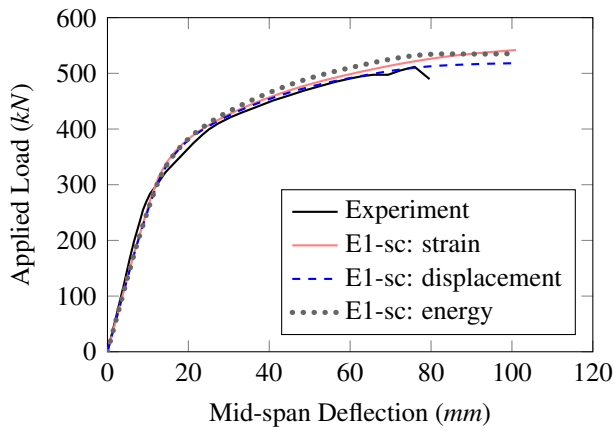


Figure 4.16: Load vs. mid-span deflection, all tension stiffening methods - beam E1-sc.

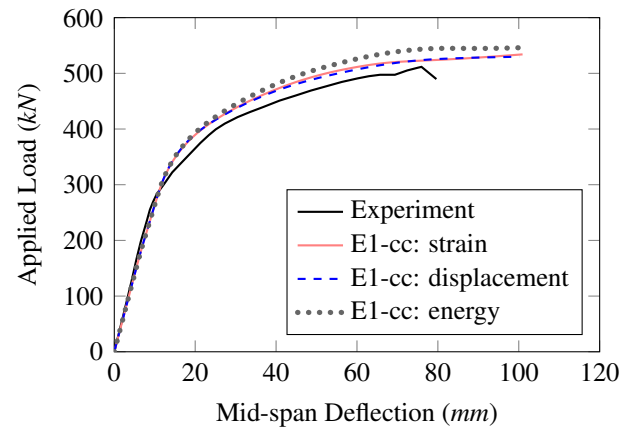


Figure 4.17: Load vs. mid-span deflection, all tension stiffening methods - beam E1-cc.

Concluding this section, it can be assumed that all three numerical models are in good agreement with experimental results. The proposed procedure can accurately predict the nonlinear behavior of the steel-concrete composite beam.

### 4.5.1 Computational effort

In Tab. 4.5 are presented the number of finite elements for each proposed specimen. The maximum size mesh for all the specimens is 45 mm. It can be easily noticed that the running time increases as more complex finite elements are used. In terms of percentage there is a difference of 30.10% between E1-sc and E1 and 201.12 % between E1-cc and E1.

Table 4.5: Number of finite elements for each proposed model

Specimen	Component	Beam B31	Shell S4R	Truss T3D2	Solid C3D8R	Job Running Time <sup>a</sup>
E1	structural steel	122				535
	concrete slab		3416			
	reinforcement					
E1-sc	structural steel		1540			696
	concrete slab				8250	
	reinforcement			2224		
E1-cc	structural steel				4392	1611
	concrete slab				9882	
	reinforcement			2488		

<sup>a</sup> Refers to the wall clock time which is largely the time taken to perform all I/O requests. The value is in (s).

Considering the computational time and effort, the number of finite elements and more important the results obtained, it can be assumed that the simple proposed procedure, using beam and shell finite elements, can be used successfully in order to evaluate the behavior of the steel-concrete composite beams with full and partial shear connection.

# Chapter 5

## Conclusions and future lines of investigations

### 5.1 Summary of the work

The present thesis is focused on steel-concrete composite beams which have seen widespread use both in modern buildings and highway bridges in recent decades due to multiple advantages that occur by combining the individual mechanical properties of the component materials, concrete and steel. Accordingly, the subject shows great importance and is still an active field of research.

Numerous experimental programs have been carried out. Some of the most important experimental tests in order to study the behavior of the steel-concrete composite beams are highlighted in the present research, such as Culver *et al.* 1961, Slutter and Driscoll Jr 1963, Chapman *et al.* 1964, Ansourian 1981, Nie and Cai 2003 and Loh *et al.* 2003a.

Also, numerical simulations have received much attention in recent years. A significant number of different procedures were developed from the simplest to the most complex. Accordingly, most of the research on steel-concrete composite beams has been focused on the development of specific finite elements with either displacement, force-based or mixed formulations. The most relevant are summarized in the present research, such as El-Lobody *et al.* 2009, Queiroz *et al.* 2007, Vasdravellis *et al.* 2012 and Chiorean 2013.

On the other hand, the design codes became richer in prescriptions and suggestions. A discussion is made upon different design codes.

In order to evaluate the behavior of the steel-concrete composite beams with full and partial shear connection, a simple numerical procedure is proposed by the author. The term *full shear connection* relates to the case in which the connection between the components is able to fully resist the forces applied. On the contrary, the situation is named *partial shear connection*. The results are validated by comparison against experimental tests, as well as against alternative numerical studies.

Therefore, several parametric studies presenting the prescriptions of different design codes in order to attain full shear connection, the influence of the concrete slab strength and the effective width of concrete slab on the structure behavior in steel-concrete composite beams, the mesh-sensitivity analysis and the fracture energy effects on the structural response of composite beams, are carried out in order to strengthen the proposed procedure.

In conclusion, taking into account the simplicity of the proposed model by means of computational time and small number of finite elements, and more important the results one can assume that the

proposed procedure, based on Abaqus software package, is a reliable and robust numerical model for steel-concrete composite beams.

### 5.2 Conclusions

The purpose of the present study was to develop a simple numerical procedure for the analysis of steel and concrete composite beams with full and partial shear connection.

In this sense, a three-dimensional finite element tool was developed based on the use of Abaqus CAE v.6.11 software package. The finite element types considered in the model are *beam* element for the structural steel and *shell* element for the concrete slab. The reinforcement is distributed over the shell element. The connection between the concrete slab and steel beam was achieved by means of connector elements. The model accounts for nonlinear behavior of concrete slab, reinforcement, structural steel and shear connectors.

The proposed procedure has been verified by comparing the predicted results with the established experimental results and also with other numerical procedures available from the literature. It was noticed that the present procedure demonstrate good capabilities of predicting the real behavior of the composite beam, in terms of nonlinear behavior and ultimate load capacity. By varying the level of shear connection, which is defined as the ratio between the shear connection capacity and the weakest element capacity, the effectiveness of the proposed procedure was demonstrated. It was observed that, increasing the number of shear connectors does not lead to significant increases in ultimate load capacity but decreasing the level of shear connection makes the system become more flexible, with reduced strength and stiffness. Also, it can be concluded that the partial shear connection has a significant influence on the deformability of the composite beams, subject that is not so well-known and is of great interest in the future research.

A set of parametric studies have been carried out in order to investigate the overall structural behavior of the composite beams. It was noticed that an increase in the concrete slab strength resulted in a stiffer system and in an increase in the moment capacity of the steel-concrete composite beam. Also, it was presented that the influence of the effective width of concrete slab on the structure behavior in a steel-concrete composite beam is significant.

A mesh sensitivity study was also undertaken, focused on the influence of the mesh size on the simulation results, which revealed that the numerical models may be insensitive to the mesh sizes and only the smoothness of the post-cracking curves are slightly influenced.

The effects of fracture energy on the steel-concrete composite beams response were also part of the parametric studies conducted. The results were not as expected, due to the fact that the concrete slab is modeled with shell finite elements. Therefore, it was necessary to develop a more complex numerical method to study these effects. In this sense, two models were developed using different types of finite elements. The structural steel and concrete slab were modeled in one procedure with *shell* and *solid* finite element types, and the other procedure both with *solid* finite element type. It was noticed that the two new proposed procedures are in good agreement with experimental results. Nevertheless, in some cases these types of procedures can be disadvantageous due to the high computational time and

effort. Therefore, it must be established the effects to be studied and with respect to this, the finite element model must be developed.

Considering the aforementioned, it can be concluded that the proposed procedure which is a simple modeling procedure with high calculation efficiency, compared to other procedures available in the literature, is a valid tool for analyzing the steel-concrete composite beams behavior with full and partial shear connection and also for extensive parametric studies.

## 5.3 Future lines of investigation

The numerical model developed and presented in this master thesis offers a great perspective in other lines of investigation. In this sense, future work is contemplated in order to investigate:

- The behavior of the partial shear connection of the composite beams subjected to uniformly distributed loading.
- The influence of the partial shear connection on the deformability of the composite beams.
- Nonlinear analysis of continuous steel-concrete composite beams taking into account the effect of partial shear connection
- Extension of the study to carry out nonlinear steel-concrete composite frameworks and, particularly study of the influence of the partial shear connection on  $2^{nd}$  order effects.
- Nonlinear analysis of steel-concrete composite frameworks considering semi-rigid connections. Study of  $2^{nd}$  order effects.
- Other parametric studies.



# Bibliography

## Books and Software user manuals

- Abaqus (2011). *Abaqus user's manual, version 6.11*. 1080 Main Street, Pawtucket, RI 02860-4847, USA: Hibbitt, Karlsson and Sorensen, Inc.
- Johnson, R. P. (2004). *Composite Structures of Steel and Concrete*. Ed. by R. Johnson. Vol. 19. 4. Oxford, UK: Blackwell Publishing Ltd, p. 338. DOI: 10.1002/9780470774625.
- Li, G.-Q. and Li, J.-J. (2007). *Advanced Analysis and Design of Steel Frames*. Chichester, UK: John Wiley & Sons, Ltd, p. 392. DOI: 10.1002/9780470319949.

## Conference Proceedings

- Buru, Ş. M., Miculaş, C. V., Şelariu, M. D., Milchiş, T., and Chiorean, C. G. (2014). “Advanced Nonlinear Inelastic Analysis of Composite Beams with Partial Shear Connection”. In: *Proceedings of the Second Conference for PhD students in Civil Engineering and Architecture*, pp. 57–59.
- Feldmann, M., Hechler, O., Hegger, J., and Rauscher, S. (2008). “Fatigue Behavior of Shear Connectors in High Performance Concrete”. In: *Composite Construction in Steel and Concrete VI*. figure 1. Reston, VA: American Society of Civil Engineers, pp. 39–51. DOI: 10.1061/41142(396)4.
- Kadlec, L. and Cervenka, V. (2015). “Uncertainty of numerical models for punching resistance of RC slabs”. In: *Concrete - Innovation and Design, fib Symposium*, pp. 1–13.
- Lam, D. and El-Lobody, E. (2011). “Finite element modelling of headed stud in composite steel beams with precast hollow core slabs”. In: *Proceedings of the First International Conference on Steel and Composite Structures*, pp. 1253–1260.
- Rauscher, S. and Hegger, J. (2008). “Modern Composite Structures Made of High Performance Materials”. In: *Composite Construction in Steel and Concrete VI*. 691. Reston, VA: American Society of Civil Engineers, pp. 691–702. DOI: 10.1061/41142(396)57.

## Design Codes

- AS-2327.1 (2003). *Australian Standard™ Composite structures Part 1: Simply supported beams*.
- AISC-LRFD (1994). *Load & Resistance Factor Design*.
- EN 1992-1-1 (2004). *Eurocode 2: Design of concrete structures - Part 1-1: General rules and rules for buildings*.
- EN 1993-1-1 (2005). *Eurocode 3: Design of steel structures - Part 1-1: General rules and rules for buildings*.
- EN 1994-1-1 (2004). *Eurocode 4: Design of composite steel and concrete structures - Part 1-1: General rules and rules for buildings*.

### Journal Articles

- Amadio, C., Fedrigo, C., Fragiaco, M., and Macorini, L. (2004). “Experimental evaluation of effective width in steel-concrete composite beams”. In: *Journal of Constructional Steel Research* 60.2, pp. 199–220. DOI: 10.1016/j.jcsr.2003.08.007.
- Amadio, C. and Fragiaco, M. (2002). “Effective width evaluation for steel-concrete composite beams”. In: *Journal of Constructional Steel Research* 58.3, pp. 373–388. DOI: 10.1016/S0143-974X(01)00058-X.
- (2003). “Analysis of rigid and semi-rigid steel-concrete composite joints under monotonic loading Part I: Finite element modelling and validation”. In: *Steel and Composite Structures* 3.5, pp. 349–369.
- Ansourian, P. (1981). “Experiments on continuous composite beams.” In: *ICE Proceedings* 73.1, pp. 26–51. DOI: 10.1680/iicep.1982.1871.
- Arrayago, I., Picci, F., Mirambell, E., and Real, E. (2015). “Interaction of bending and axial load for ferritic stainless steel RHS columns”. In: *Thin-Walled Structures* 91, pp. 96–107. DOI: 10.1016/j.tws.2015.02.012.
- Baskar, K., Shanmugam, N. E., and Thevendran, V. (2002). “Finite-Element Analysis of Steel-Concrete Composite Plate Girder”. In: *Journal of Structural Engineering* 128.9, pp. 1158–1168. DOI: 10.1061/(ASCE)0733-9445(2002)128:9(1158).
- Brühwiler, E. and Wittmann, F. H. (1990). “The wedge splitting test, a new method of performing stable fracture mechanics tests”. In: *Engineering Fracture Mechanics* 35.1-3, pp. 117–125. DOI: 10.1016/0013-7944(90)90189-N.
- Bursi, O. S. and Gramola, G. (2000). “Behaviour of composite substructures with full and partial shear connection under quasi-static cyclic and pseudo-dynamic displacements”. In: *Materials and Structures* 33.3, pp. 154–163. DOI: 10.1007/BF02479409.
- Bursi, O. S., Sun, F. F., and Postal, S. (2005). “Non-linear analysis of steel-concrete composite frames with full and partial shear connection subjected to seismic loads”. In: *Journal of Constructional Steel Research* 61.1, pp. 67–92. DOI: 10.1016/j.jcsr.2004.06.002.
- Chapman, J. C. and Balakrishnan, S. (1964). “Experiments on composite beams”. In: *The Structural Engineer* 42.1, pp. 369–383.
- Chiorean, C. G. (2013). “A computer method for nonlinear inelastic analysis of 3D composite steel-concrete frame structures”. In: *Engineering Structures* 57, pp. 125–152. DOI: 10.1016/j.engstruct.2013.09.025.
- Culver, C. and Coston, R. (1961). “Tests of composite beams with stud shear connectors”. In: *ASCE Journal of Structural Division* 87.174, pp. 1–17.
- Dezi, L., Gara, F., Leoni, G., and Tarantino, A. M. (2001). “Time-Dependent Analysis of Shear-Lag Effect in Composite Beams”. In: *Journal of Engineering Mechanics* 127.1, pp. 71–79. DOI: 10.1061/(ASCE)0733-9399(2001)127:1(71).
- Gattesco, N. (1999). “Analytical modeling of nonlinear behavior of composite beams with deformable connection”. In: *Journal of Constructional Steel Research* 52.2, pp. 195–218. DOI: 10.1016/S0143-974X(99)00026-7.
- Gattesco, N. and Giuriani, E. (1996). “Experimental Study on Stud Shear Connectors Subjected to Cyclic Loading”. In: *Journal of Constructional Steel Research* 38.1, pp. 1–21. DOI: 10.1016/0143-974X(96)00007-7.
- Gil, B. and Bayo, E. (2008). “An alternative design for internal and external semi-rigid composite joints. Part II: Finite element modelling and analytical study”. In: *Engineering Structures* 30.1, pp. 232–246. DOI: 10.1016/j.engstruct.2007.03.010.
- Hillerborg, A., Modéer, M., and Petersson, P.-E. (1976). “Analysis of crack formation and crack growth in concrete by means of fracture mechanics and finite elements”. In: *Cement and Concrete Research* 6.6, pp. 773–781. DOI: 10.1016/0008-8846(76)90007-7.



- Hradil, P., Fülöp, L., and Talja, A. (2012). “Global stability of thin-walled ferritic stainless steel members”. In: *Thin-Walled Structures* 61, pp. 106–114. DOI: 10.1016/j.tws.2012.05.006.
- Kim, H.-Y. and Jeong, Y.-J. (2010). “Ultimate strength of a steel–concrete composite bridge deck slab with profiled sheeting”. In: *Engineering Structures* 32.2, pp. 534–546. DOI: 10.1016/j.engstruct.2009.10.014.
- Lam, D. and El-Lobody, E. (2001). “Finite element modelling of headed stud shear connectors in steel-concrete composite beam”. In: *Structural Engineering, Mechanics and Computation*, pp. 401–408.
- Lam, D. and El-Lobody, E. (2005). “Behavior of Headed Stud Shear Connectors in Composite Beam”. In: *Journal of Structural Engineering* 131.1, pp. 96–107. DOI: 10.1061/(ASCE)0733-9445(2005)131:1(96).
- El-Lobody, E. and Lam, D. (2009). “Finite Element Analysis of Steel-Concrete Composite Girders”. In: *Advances in Structural Engineering* 6.4, pp. 267–281. DOI: 10.1260/136943303322771655.
- Loh, H., Uy, B., and Bradford, M. (2004). “The effects of partial shear connection in the hogging moment regions of composite beams”. In: *Journal of Constructional Steel Research* 60.6, pp. 897–919. DOI: 10.1016/j.jcsr.2003.10.007.
- Mistakidis, E. S., Thomopoulos, K., Avdelas, A., and Panagiotopoulos, P. D. (1994). “Shear connectors in composite beams: A new accurate algorithm”. In: *Thin-Walled Structures* 18.3, pp. 191–207. DOI: 10.1016/0263-8231(94)90018-3.
- Nguyen, Q. H., Hjiat, M., Uy, B., and Guezouli, S. (2009). “Analysis of composite beams in the hogging moment regions using a mixed finite element formulation”. In: *Journal of Constructional Steel Research* 65.3, pp. 737–748. DOI: 10.1016/j.jcsr.2008.07.026.
- Nie, J. and Cai, C. (2003). “Steel–Concrete Composite Beams Considering Shear Slip Effects”. In: *Journal of Structural Engineering* 129.April, pp. 495–506. DOI: 10.1061/(ASCE)0733-9445(2003)129:4(495).
- Nie, J., Cai, C., Zhou, T., and Li, Y. (2007). “Experimental and Analytical Study of Prestressed Steel–Concrete Composite Beams Considering Slip Effect”. In: *Journal of Structural Engineering* 133.4, pp. 530–540. DOI: 10.1061/(ASCE)0733-9445(2007)133:4(530).
- Nie, J., Tao, M., Cai, C., and Chen, G. (2011). “Modeling and investigation of elasto-plastic behavior of steel-concrete composite frame systems”. In: *Journal of Constructional Steel Research* 67, pp. 1973–1984. DOI: 10.1016/j.jcsr.2011.06.016.
- Oehlers, D. J., Nguyen, N. T., Ahmed, M., and Bradford, M. A. (1997). “Partial interaction in composite steel and concrete beams with full shear connection”. In: *Journal of Constructional Steel Research* 41.2-3, pp. 235–248. DOI: 10.1016/S0143-974X(97)80892-9.
- Ollgaard, J. G., Slutter, R. G., and Fisher, J. W. (1971). “Shear strength of stud connectors in lightweight and normal weight concrete”. In: *AISC Engineering Journal* 8, pp. 55–64.
- Papastergiou, D. and Lebet, J.-P. (2014). “Design and experimental verification of an innovative steel–concrete composite beam”. In: *Journal of Constructional Steel Research* 93, pp. 9–19. DOI: 10.1016/j.jcsr.2013.10.017.
- Pi, Y.-L., Bradford, M. A., and Uy, B. (2006). “Second Order Nonlinear Inelastic Analysis of Composite Steel–Concrete Members. II: Applications”. In: *Journal of Structural Engineering* 132.5, pp. 762–771. DOI: 10.1061/(ASCE)0733-9445(2006)132:5(762).
- Queiroz, F. D., Vellasco, P. C. G. S., and Nethercot, D. A. (2007). “Finite element modelling of composite beams with full and partial shear connection”. In: *Journal of Constructional Steel Research* 63.4, pp. 505–521. DOI: 10.1016/j.jcsr.2006.06.003.
- Razaqpur, A. G. and Nofal, M. (1989). “A finite element for modelling the nonlinear behavior of shear connectors in composite structures”. In: *Computers & Structures* 32.1, pp. 169–174. DOI: 10.1016/0045-7949(89)90082-5.

## Bibliography

---

- Sedlacek, G. and Bild, S. (1993). "A simplified method for the determination of the effective width due to shear lag effects". In: *Journal of Constructional Steel Research* 24.3, pp. 155–182. DOI: 10.1016/0143-974X(93)90042-Q.
- Slutter, R. G. and Driscoll Jr, G. C. (1963). "The flexural strength of steel and concrete composite beams". In: December.
- Slutter, R. G. and Fisher, J. W. (1965). "Tentative design procedure for shear connectors in composite beams". In: 316, p. 22.
- (1966). "Fatigue Strength of Shear Connectors". In: *45th Annual Meeting of the Highway Research Board* 147.
- Vasdravellis, G., Uy, B., Tan, E. L., and Kirkland, B. (2012). "Behaviour and design of composite beams subjected to negative bending and compression". In: *Journal of Constructional Steel Research* 79, pp. 34–47. DOI: 10.1016/j.jcsr.2012.07.012.
- Zona, A. and Ranzi, G. (2011). "Finite element models for nonlinear analysis of steelconcrete composite beams with partial interaction in combined bending and shear". In: *Finite Elements in Analysis and Design* 47.2, pp. 98–118. DOI: 10.1016/j.finel.2010.09.006.

## Technical Reports

- Hognestad, E. (1951). *Study of combined bending and axial load in reinforced concrete members*. Tech. rep. Bulletin Series No. 399. Chicago: University of Illinois.
- Loh, H., Uy, B., and Bradford, M. (2003a). *The behaviour of composite beams in hogging moment regions, part I - experimental study*. Tech. rep. Uniciv Report No. 418. Sydney: The University of New South Wales - School of Civil and Environmental Engineering.
- (2003b). *The behaviour of composite beams in hogging moment regions, part II - analytical study*. Tech. rep. Uniciv Report No. 419. Sydney: The University of New South Wales - School of Civil and Environmental Engineering.